FULL PAPER

Synthesis, Linear, and Quadratic-Nonlinear Optical Properties of Octupolar D_3 and D_{2d} Bipyridyl Metal Complexes

Olivier Maury,[a] Lydie Viau,[a] Katell Sénéchal,[a] Brigitte Corre,[a] Jean-Paul Guégan,[a] Thierry Renouard,[a] Isabelle Ledoux,[b] Joseph Zyss,[b] and Hubert Le Bozec*[a]

Abstract: A series of D_3 (Fe^{II}, Ru^{II}, Zn^{II}, Hg^{II}) and D_{2d} (Cu^I, Ag^I, Zn^{II}) octupolar metal complexes featuring different functionalized bipyridyl ligands has been synthesized, and their thermal, linear (absorption and emission), and nonlinear optical (NLO) properties were determined. Their quadratic NLO susceptibilities were determined by harmonic light scattering at 1.91 μm, and the molecular hyperpolarizability (β_0) values are in the range of 200–657×10^{-30} esu for octahedral complexes and 70–157×10^{-30} esu for tetrahedral complexes. The octahedral zinc(II) complex **1e**, which contains a 4,4′-oligophenylenevinylene-functionalized 2,2′-bipyridine, exhibits the highest quadratic hyperpolarizability ever reported for an octupolar derivative ($\lambda_{max} = 482$ nm, $\beta^{1.91}(\mathbf{1e}) = 870 \times 10^{-30}$ esu, $\beta_0(\mathbf{1e}) = 657 \times 10^{-30}$ esu). Herein, we demonstrate that the optical and nonlinear optical (NLO) properties are strongly influenced by the symmetry of the complexes, the nature of the ligands (donor endgroups and π linkers), and the nature of the metallic centers. For example, the length of the π-conjugated backbone, the Lewis acidity of the metal ion, and the increase of ligand-to-metal ratio result in a substantial enhancement of β. The contribution of the metal-to-ligand (MLCT) transition to the molecular hyperpolarizability is also discussed with respect to octahedral d^6 complexes (M = Fe, Ru).

Keywords: absorption · coordination chemistry · fluorescence · ligand design · N ligands · nonlinear optics

Introduction

Interest in nonlinear optics has led to the design of chromophores with a large molecular hyperpolarizability, mainly one-dimensional (1D) dipolar chromophores.[1] Beyond this classical approach, the concept of octupolar nonlinearities was proposed at the beginning of the nineties on the basis of group theoretical and quantum mechanical calculations.[2] For molecules belonging to octupolar space groups, the vector part of the molecular hyperpolarizability $\beta_{(J=1)}$ is cancelled so that only the octupolar contribution $\beta_{(J=3)}$ remains.

The archetype of the octupolar structure is a cube with alternating donor and acceptor groups at the edges (Figure 1).[2] Basically, purely octupolar symmetries can be derived from this cubic T_d structure either by projection along a C_3 axis, giving rise to D_{3h} or D_3 symmetry ("TATB route"), or by fusion of one type of charge in the barycenter leading to D_{3h}, D_3, T_d, or D_{2d} symmetry ("guanidinium route") (Figure 1). Thus, the molecular engineering of octupoles consists of a spatially controlled organization of charge transfers within a molecule in order to reach the desired symmetry.

Most octupolar systems developed to date are organic molecules.[3] They have been designed by chemical functionalization of a central core and can be roughly classified into three main classes: 1) 2D molecules of global D_{3h} symmetry obtained by 1,3,5-functionalization of a central aromatic core (phenyl,[4] triazine,[5] or boroxine[6]); 2) D_{3h} or slightly twisted D_3 propeller-like molecules, such as functionalized trivalent carbon (carbocation, carbanion, or radical),[7] or nitrogen atoms;[8] and 3) three-dimensional tetrahedral (T_d) molecules, such as tetrasubstituted carbon,[9] phosphonium,[10] or tin[11] derivatives. Other examples of octupolar structures, such as subphthalocyanines,[12] O,O'-functionalized biphenyl derivatives,[13] cryptands,[14] and paracyclophanes,[15] have also been described recently.
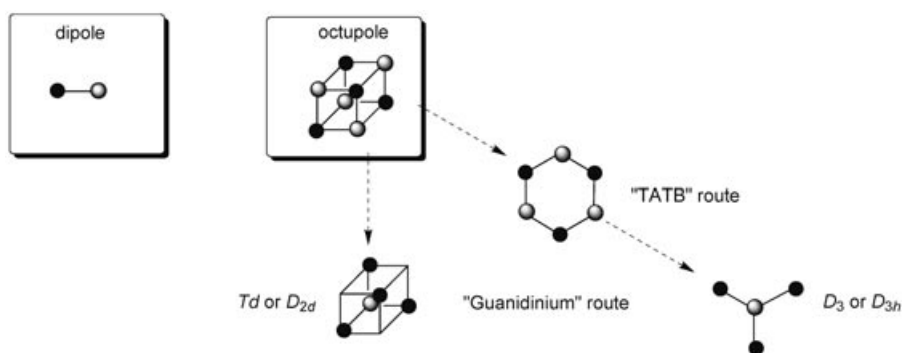
Figure 1. Archetype of second-order NLO-active structures.

cal properties (β) of a versatile family of D_3 (Fe^{II}, Ru^{II}, Zn^{II}, Hg^{II}) and D_{2d} (Cu^I, Ag^I, Zn^{II}) octupolar metal complexes that feature different functionalized bipyridyl ligands. The main objective of this work is to investigate the relationships between molecular hyperpolarizabilities (β) and molecular structures by the use of various ligand/metal combinations. We demonstrate the influence of molecular parameters, such as the nature of the donor group and the π-conjugated backbone, on the absorption (ILCT) and NLO properties. We discuss the key role of the central metal ion as a versatile template and Lewis acid for the design of highly NLO-active octupoles. The intriguing dual role of the MLCT and ILCT transitions in d^6 octahedral complexes, both of which can contribute to the molecular hyperpolarizability (β) is also examined.

Coordination chemistry can also be an alternative way and a powerful tool to build up octupolar arrangements. The first demonstration of the potential of transition-metal complexes for NLO was reported by Zyss who used [Ru(bpy)$_3$]$^{2+}$, which has D_3 symmetry.[16] Following this work, a variety of octupolar NLO-phores based on metal complexes have been designed and investigated, especially by Lin[17] and our group.[18] We have been essentially concerned with the NLO properties of 4,4′-disubstituted 2,2′-bipyridine metal complexes. An interesting feature offered by these ligands is their synthetic flexibility that allows fine-tuning of the optical properties by simple modification of the π-conjugated backbone.[19] These ligands are excellent building blocks for the construction of either octahedral[18a] or pseudotetrahedral octupolar complexes.[18b] In these systems, the metal plays two important roles that both contribute to NLO activity: 1) it is a powerful template to gather ligands in a predetermined octupolar arrangement, and 2) it acts as a Lewis acid to induce a strong intraligand charge transfer (ILCT) transition.

Herein, we describe in detail the synthesis and the thermal, optical (absorption and emission), and nonlinear opti-

Results and Discussion

Octahedral D_3 symmetric octupolar complexes: Figure 2 depicts the generic structure of the D_3 octahedral metallo-octupoles and the different parameters that have been examined in this study. The synthesis of the "push-pull" bipyridyl chromophores bearing alkoxy (**a**) or amino (**b**) donor groups and different π-conjugated backbones (**b**: styryl, **c**: thienylvinyl), was described elsewhere.[19] Bipyridine **d**, which contains two phenylimino moieties, was prepared in 85% yield by a Schiff-base condensation between 4,4′-diformyl-2,2′-bipyridine[20] and N,N-dibutyl-1,4-phenylenediamine. Bipyridine **e**, which features a bistyryl linker, was synthesized by means of a double Wadworth–Emmons condensation between 4,4′-bis(diethylphosphonatomethyl)-2,2′-bipyridine and p-dibutylaminostyrylbenzaldehyde (see the Experimental Section).[21]

The metal complexes [M = Zn (**1**), Ru (**2**), Fe (**3**), Hg (**4**)] of these ligands were prepared in good yields by refluxing three equivalents of the bipyridine (**a–d**) with the metallic precursors ([RuCl$_2$(dmso)$_4$], ZnOAc$_2$·2H$_2$O, FeCl$_2$·4H$_2$O, HgCl$_2$) in ethanol, followed by an anionic metathesis with sodium hexafluorophosphate (Scheme 1). Owing to the poor solubility of **e**, the corresponding zinc complex **1e** was isolated with the tris(tetrachlorobenzenediolato)phosphate (TRISPHAT) counterion, which is known to significantly improve the solubility.[22] The preparation of [M(**a**)$_3$][PF$_6$]$_2$ (M = Zn, Fe) led to the formation of an unclean mixture of complexes in which a partial trans–cis isomerization of the styryl double bond could be observed. To overcome this problem, an anionic exchange from PF$_6$$^-$ to TRISPHAT was carried out in dichloromethane. The resulting complexes **1a** and **3a** could then be isolated as their pure trans isomer (vide infra) in modest yields after flash column chromatography (silica gel, CH$_2$Cl$_2$). This behavior was in marked con-

Abstract in Breton: *Sintezekaet zo bet ur familh kemplezhioù metalek eizhpol, enno ligantoù daoubiridin arc'hwelekaet. O ferzhioù termek, optik linennek (euvriñ ha skingas) hag anlinennek zo bet termenet. Oberiegezh optikel anlinennek ar c'hediadoù-se zo bet gallet termeniñ gant teknik skignañ harmonek ar sklêrijenn diouzh un hirder gwagennoù a 1.91 μm: talvoudegezhioù arβ$_0$ zo etre 200 ha 657×10^{-30} ues evit ar c'hemplezhioù eizhtalek hag etre 70 ha 157×10^{-30} ues evit ar c'hemplezhioù pevarzalek. Gant ar c'hediad zink(II) 1 añ emañ an oberiegezh anlinennek eil-urzh kreñvañ a vefe bet a-viskoazh evit ur volekulenn eizhpol. Gant ar studiadenn-mañ eo sklaer pegen levezonet eo ar perzhioù optik linennek hag anlinennek gant simetriezh ar molekul, anien al ligantoù (anien ar roer hag ar reizhiad treuzkas) hag anien ar c'hreiz metalek. Da skouer, gant hirder ar chadenn kediet, trenkted Lewis ar metal ha kresk ar c'heñver ligant/metal e kresk kalz ar β$_0$. Mod-all ez eus bet lakaet sklaer e ro an MLCT harp d'an oberiegezh optik anlinennek er c'hemplezhioù eizhtalek d^6.*
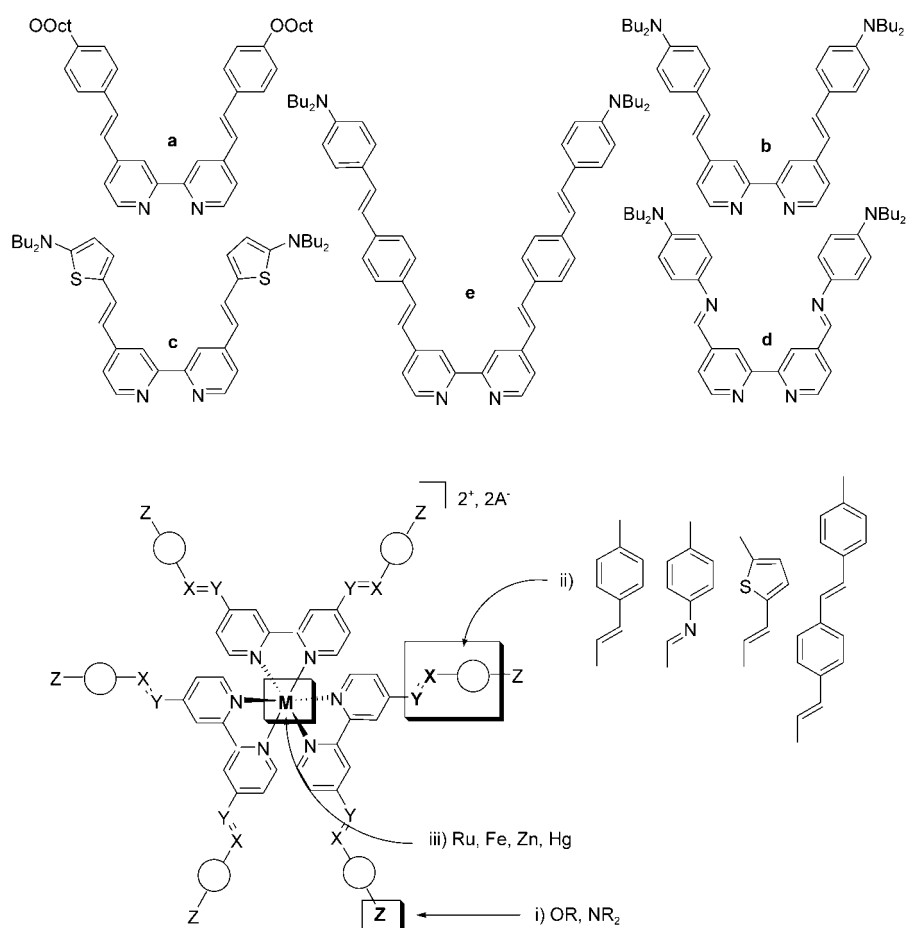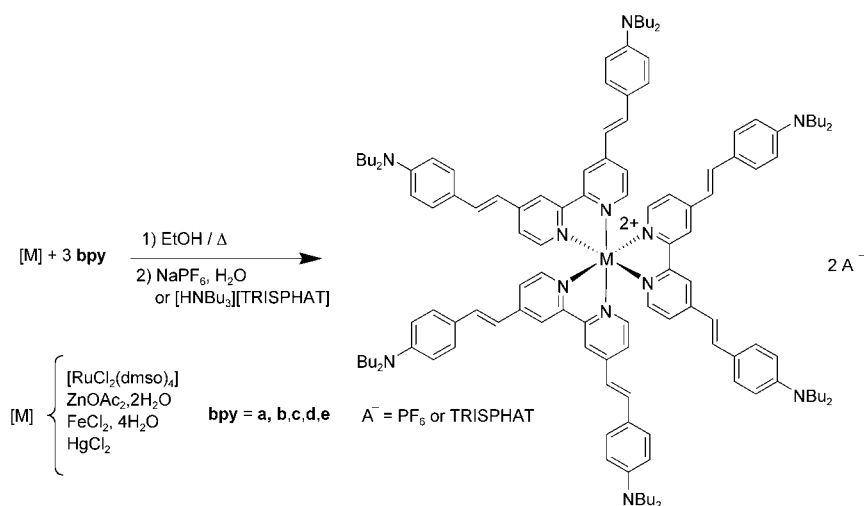
Figure 2. Generic structure of the D_3-symmetric family of metallo-octupoles.

Scheme 1. Synthesis of D_3 metallo-octupoles.

nals is observed, as expected for highly symmetric D_3 complexes. For all complexes, the ^{1}H NMR spectra exhibit a characteristic AB system for the alkenyl protons H7 and H8 with a ^3J(H7,H8) coupling constant of ≈ 16 Hz, which is indicative of E configuration (see Figure 9 in the Experimental Section for the numbering). A significant upfield shift of the H6 protons is observed upon complexation and the magnitude of this shift is strongly dependant on the nature of the metal. For example, in the series [M(**b**)$_3$][PF$_6$]$_2$, $\Delta\delta$(H6) $= -0.31$, -0.76, -0.97, and -1.19 ppm (M = Hg, Zn, Ru, Fe, respectively). The same trend is observed with the [M(**a**)$_3$][TRISPHAT]$_2$ series. In addition, as already observed, replacement of PF$_6^-$ by TRISPHAT results in a downfield shift of the H6 proton ($\approx$ 0.6 ppm), as a consequence of homochiral self-assembly between both propeller-like D_3 symmetric anions and dications.[22b]

The thermal stabilities of complexes **1–3** (Td$_{10}$ corresponds to the 10% weight-loss temperature), were determined by TGA under nitrogen (Table 1). The thermal stability of these tris(bipyridyl) metal complexes is slightly less than the corresponding ligands. For example, thermal decomposition of complexes containing the most stable ligand **b** (Td$_{10}$(**b**) = 380°C) occurs between 385 and 330°C. For both series [M(**a**)$_3$]$^{2+}$ and [M(**b**)$_3$]$^{2+}$, the thermal stability follows the same tendency, namely, Ru > Fe > Zn. Complexes featuring styryl–bipyridine derivatives appear to be the most thermally robust chromophores, comparable to the highest thermal stability reported in the literature.[23] In contrast, **1c** and **1d** are very unstable and decompose immediately upon heating (Td$_{10}$ < 50°C), or even at room temperature when conserved in a flask for a few weeks. This strong instability prevented their characterization by elemental analysis and only the stable complexes **1–3a,b,e** gave satisfactory microanalyses. In addition, further

trast to that of [Ru(**a**)$_3$]$^{2+}$ (**2a**), which could be isolated either as its hexafluorophosphate or TRISPHAT salt.

All complexes were unambiguously characterized by means of ^{1}H, ^{13}C NMR, UV-visible, and fluorescence spectroscopy, high-resolution mass spectrometry, and a satisfactory elemental analysis. ^{1}H and ^{13}C NMR spectra are in agreement with the proposed structures: only one set of sig-

Table 1. Linear and nonlinear optical data of D_3 and D_{2d} metallo-octupoles.

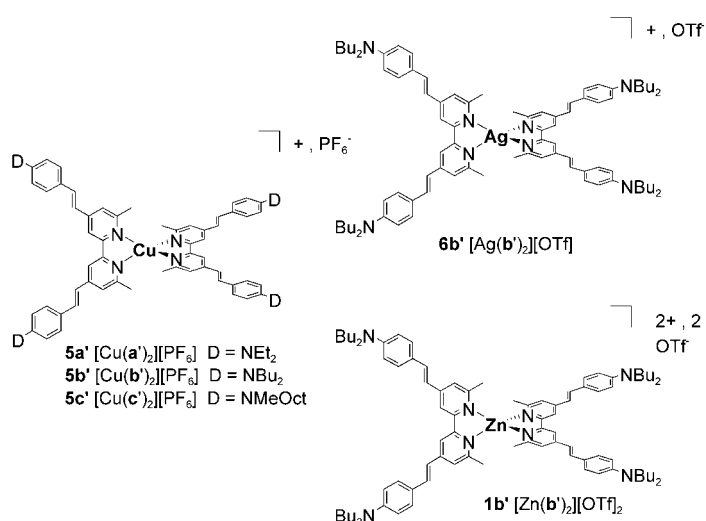| Complexes		λ_{max} [nm][a]	ε [L mol⁻¹ cm⁻¹]	$\Delta\lambda$ [nm][b]	λ_{em} [nm][a]	$\beta^{1.34}$ [10⁻³⁰ esu][c]	$\beta^{1.91}$ [10⁻³⁰ esu][c]	β_0 [10⁻³⁰ esu][d]	Td_{10} [°C]
[Zn(**a**)₃][TRISPHAT]₂	**1a**	382	128000	45	501		250	200	335
[Zn(**b**)₃][PF₆]₂	**1b**	466	175000	65	644	940	340	240	330
[Zn(**c**)₃][PF₆]₂	**1c**	519	50000	76	—[e]		400	260	decomp
[Zn(**d**)₃][PF₆]₂	**1d**	506	68000	73	no		310	207	decomp
[Zn(**e**)₃][TRISPHAT]₂	**1e**	482	132000	62	no		870	657	285
[Ru(**a**)₃][TRISPHAT]₂	**2a**	387	124000	50	678		270	—[g]	365
		510	51000						
[Fe(**a**)₃][TRISPHAT]₂	**3a**	382	141000	45	500		220	—[g]	360
		583	41000						
[Ru(**b**)₃][PF₆]₂	**2b**	446	142000	45	721	1130	340	—[g]	385
		520	150000						
[Fe(**b**)₃][PF₆]₂	**3b**	467	168000	66	645	256	235	—[g]	350
		593	75000						
[Hg(**b**)₃][PF₆]₂	**4b**	438	160000	37	621	515			
[Cu(**a'**)₂][PF₆]	**5a'**	433	83000						
		480	40000	42	—[e]				—[e]
[Cu(**b'**)₂][PF₆]	**5b'**	436	106000						
		480	45000	39	620	144	113	86	340
[Cu(**c'**)₂][PF₆]	**5c'**	420	74000						
		480	37000	34	—[e]	128		70	—[e]
[Ag(**b'**)₂][OTf]	**6b'**	431	115000	34	562		90	70	295
[Zn(**b'**)₂][OTf]₂	**1b'**	529	125000	132	no		245	157	305
[Zn(**b**)Cl₂]		459	62000	58	624	172[f]		62	395

[a] Measured in dilute CH_2Cl_2 solution (10^{-5} mol L⁻¹). [b] Difference between the λ_{max} of the complex and that of the corresponding ligand. [c] Measured by HRS (precision ±15%) in concentrated CH_2Cl_2 solution ($1–5\times10^{-3}$ mol L⁻¹). [d] Deduced from the two-level model on the basis of the $\beta^{1.91}$ values. [e] Not measured. [f] Measured by EFISH (precision ±15%) at 1.34 μm in a 10^{-3} mol L⁻¹ chloroform solution; $\mu\beta = 1830\times10^{-30}$ esu with $\mu = 10.65$ D. [g] β_0 value not determined on account of the presence of two different ILCT and MLCT transitions.
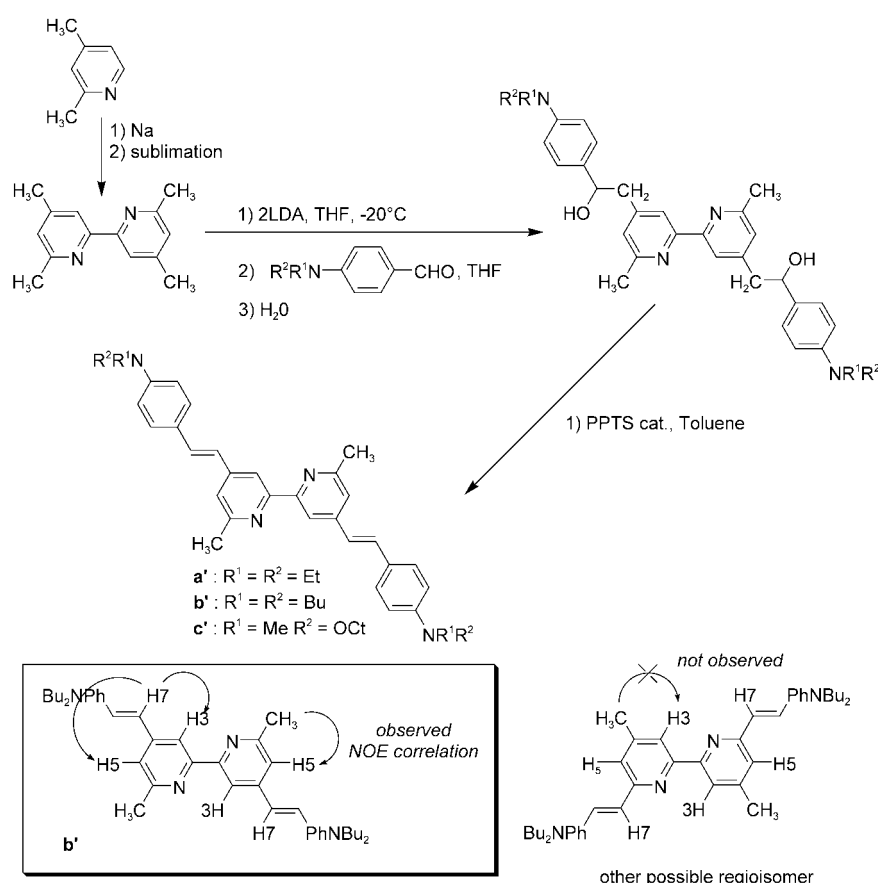
characterization by HRMS was precluded owing to decomposition in the matrix (*m*-nitrobenzylic alcohol): only the [(bipy)₂ZnF]⁺ fragment, resulting from a fluorine transfer from PF_6^-, was observed.[24]

Tetrahedral D_{2d} symmetric octupolar complexes: Bipyridyl ligands also allow the design of D_{2d} tetrahedral octupoles by coordination of two bipyridines to metal ions, such as Cu^I, Ag^I or Zn^{II}. This type of geometry has been extensively used to design new architectures that feature an original topology, such as catenates or knots.[25] The key feature to stabilize the tetrahedral geometry, and to protect the central metal ion against oxidation in the case of copper(ɪ), is the incorporation of either alkyl or aryl substituents at the 6,6′-positions in the bipyridyl ligand. The synthesis of such ligands can be easily achieved by a controlled functionalization of the 4,4′-positions in 4,4′,6,6′-tetramethyl-2,2′-bipyridine. Thus, dilithiation with LDA in THF at −20°C, followed by reaction with two equivalents of dialkylaminobenzaldehydes afforded the 4,4′-dialcohols selectively, and subsequent dehydration in the presence of a catalytic amount of pyridinium *p*-toluene sulfonate (PPTS) yielded the desired bipyridyl ligands **a′**, **b′**, and **c′** in good yields (Scheme 2).[18b] The regioselectivity of the reaction was clearly established on the basis of a ¹H NMR 2D NOESY experiment in the case of **b′**, which revealed a through-space correlation between the vinylic H7 proton and the pyridinic H3 and H5 protons (Scheme 2). A strong NOE was also observed between the methyl groups and the H5,5′ protons (but not between CH3 and H3,3′), thus confirming the proposed structure. Introduction of a methyl group in the 6,6′-positions does not induce any modification of the absorption or emission properties, or the thermal stability: like their parent ligand **b**,[19] **a′**, **b′**, and **c′** show a typical ILCT transition at ≈390 nm, a broad emission at ≈500 nm, and a thermal stability at ≈350°C (see the Experimental Section).

Red-orange copper(ɪ), silver(ɪ), and violet zinc(ɪɪ) complexes **5a′–c′**, **6b′**, and **1b′** were easily prepared by treatment of [Cu(CH₃CN)₄][PF₆], AgOTf and Zn(OTf)₂ with two equivalents of ligand **a′**, **b′**, or **c′** in dichloromethane at room temperature. These compounds were fully characterized by ¹H, ¹³C NMR, UV-visible, and fluorescence spectroscopy, microanalysis, and high-resolution mass spectrometry. ¹H

5a' [Cu(**a'**)₂][PF₆] D = NEt₂
5b' [Cu(**b'**)₂][PF₆] D = NBu₂
5c' [Cu(**c'**)₂][PF₆] D = NMeOct

6b' [Ag(**b'**)₂][OTf]

1b' [Zn(**b'**)₂][OTf]₂

Scheme 2. Synthesis and determination of the regioselectivity by means of the NOE correlation.

and ^{13}C NMR spectra are in agreement with the proposed structures: they exhibit only one set of signals, as expected for D_{2d} symmetric complexes. It is noteworthy that complexation induces a downfield shift of the H3 and H5 protons and an upfield shift of the methyl protons.[26] The magnitude of this shift correlates to the nature of the metal.[27] The stronger H3 and H5 deshielding in the case of zinc(II) ($\Delta\delta_{H5}(\mathbf{1b'}$ vs $\mathbf{b'})=0.58$ ppm) as compared to that of copper(I) or silver(I) ($\Delta\delta_{H5}\approx 0.2–0.3$ ppm) is clearly caused by the electroattractive inductive effect of the stronger Lewis acid Zn^{2+}. The upfield shift of the methyl groups comes from the aromatic ring current interaction between one ligand and the methyl group of a second, and is related to geometrical constraint with, as expected, the smaller Cu^I or Zn^{II} ions inducing the stronger upfield shift ($\Delta\delta_{CH3}=0.45$, 0.36, and 0.09 ppm for Cu, Zn, and Ag, respectively). These complexes are also fairly thermally stable (Table 1) with $305 < Td_{10} < 340$ °C.

Linear optical properties: All complexes exhibit strong absorption bands in the visible region. These bands are sensitive to the nature of the donor group, the π-conjugated backbone, and the metallic core (Table 1). Two types of transitions can be observed: intraligand charge transfer (ILCT) and metal-to-ligand charge transfer (MLCT). The influence of the nature of the ligand on the absorption properties of the related complexes has been investigated in the case of zinc(II) complexes **1a–e**, which contain alkoxy or

amino donor groups and styryl, phenylimino, thienylvinyl, or distyryl transmitters, respectively. UV-visible spectra exhibit a broad intense absorption band assigned to the ILCT transition. No MLCT transition is observed, as expected from the high third-ionization potential of zinc. Upon coordination, the acceptor strength of the pyridinic ring is enhanced, resulting in a bathochromic shift of the ILCT transition. For a given donor group, such as dibutylamino, a red shift of ≈ 70 nm is observed for the Zn^{II} series. Moreover, the energy of this transition steadily decreases when changing the styryl linkage to a distyryl, phenylimino, or thienylvinyl linkage, respectively, as found with the corresponding bipyridyl ligands (Table 1). The influence of the central metallic ion on the linear optical data of the $[M(bpy)_3]^{2+}$ series (M = Ru, Zn, Fe, Hg) was examined by using the same bipyridyl ligand (**a** or **b**). The red shift of the ILCT transition, induced by complexation, can be correlated to the Lewis acidity of the metallic ion. While the λ_{ILCT} values of the Ru^{II}, Zn^{II}, and Fe^{II} complexes are roughly similar (Figure 3), that of the Hg^{II} complex decreases significantly, in agreement with the relative Lewis acidity of these metal ions.[28] The influence of the central metallic ion on λ_{ILCT} is also clearly found for the tetrahedral series $[M(\mathbf{b'})_2]^{n+}$ ($M^{n+}=Cu^+$, Ag^+, and Zn^{2+}) (Figure 4). The λ_{ILCT} values decrease with the relative Lewis acidity in the order $Zn^{2+}\gg Cu^+>Ag^+$.
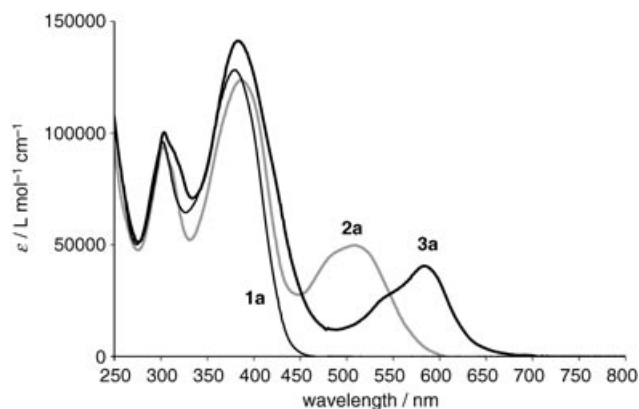

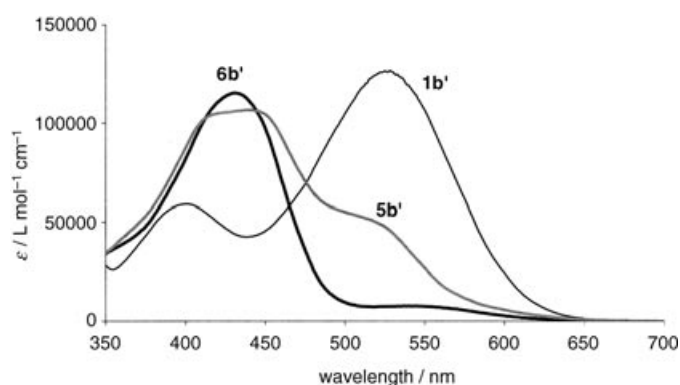Figure 3. UV-visible spectra of complexes **1a** (black), **2a** (gray) and **3a** (bold).

Figure 4. UV-visible spectra of tetrahedral complexes Cu^{I} **5b′** (gray), **6b′** (bold) Zn^{II}, **1b′** (dark).

Tris(bipyridyl) ruthenium **2a,b** and iron complexes **3a,b** each show another absorption band arising from the dπ(Ru^{II} or Fe^{II})→π*(bpy) metal-to-ligand charge-transfer (MLCT) transition. The MLCT bands of Fe^{II} complexes ($\lambda_{MLCT}\approx$ 590 nm) are usually found at longer wavelengths than those of the corresponding Ru^{II} complexes ($\lambda_{MLCT}\approx$510 nm) (Figure 3 and Table 1).[29] The UV-visible spectrum of **2b** exhibits a very broad band with two maxima at 446 and 513 nm that correspond to the overlap of the ILCT and MLCT transitions (Figure 5). The assignment of the transi-
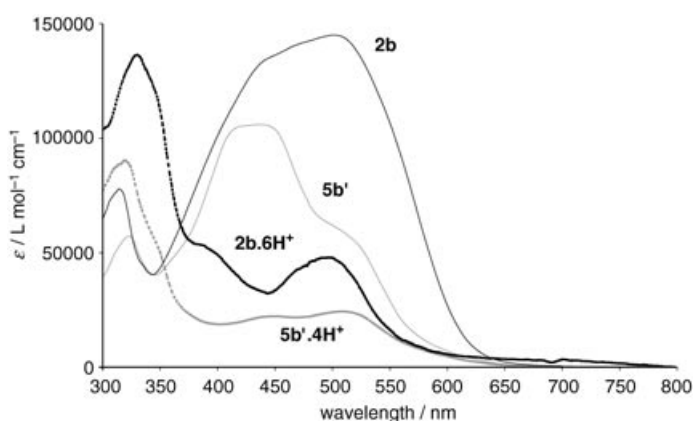

Figure 5. Acid addition experiments on **2b** (dark) and **5b′** (gray).

tions was confirmed by an acid addition experiment:[30] protonation with six equivalents of *p*-toluenesulfonic acid (PTSA) in a solution of **2b** in dichloromethane at room temperature caused a rapid color change from deep red to clear orange. The reversibility of the reaction was demonstrated by addition of a strong base (DABCO), which quantitatively regenerated the starting complex **2b** (Figure 5). Protonation of the dibutylamino groups leads to the disappearance of the ILCT band at 446 nm and the concomitant formation of a new band at a higher energy (λ(**2b**·6H$^+$) = 333 nm), which can be assigned to a ligand-centered transition. In contrast, only a small shift of the MLCT transition is observed (λ_{MLCT}(**2b**·6H$^+$) = 496 nm). The weak dependence of the MLCT transition towards the 4,4′-substituents of the bipyridyl ligands is corroborated by comparing the λ_{MLCT}

of a series of Ru^{II} complexes that feature ligands such as 4,4′-bis(octyloxystyryl)-2,2′-bipyridine **2a** (λ_{MLCT}=510 nm, ε=51 000 Lmol^{-1}cm^{-1}), 4,4′-bis(nitrostyryl)-2,2′-bipyridine (λ_{MLCT}=487 nm, ε=42 000 Lmol^{-1}cm^{-1}),[31] or 4,4′-bis(styryl)-2,2′-bipyridine (λ_{MLCT}=487 nm, ε=33 000 Lmol^{-1}cm^{-1}).[32] In the tetrahedral Cu^{I}, Ag^{I}, and Zn^{II} series, only Cu^{I} complexes show MLCT transitions that partially overlap with the ILCT transition. Again, an acid addition experiment was carried out with complex **5b′** (Figure 5) that resulted in a blue shift of the intraligand transition to 322 nm while the two MLCT transitions remained at 446 and 508 nm.[33]

Photoluminescence is observed for the bis- and tris(bipyridyl) complexes **1–4a,b**, **5–6b′** in dilute dichloromethane solution (Table 1). Zinc(II) complexes **1a,b** exhibit a broad, intense structureless emission band assigned to ligand-centered emission with very large Stokes shifts (6287 and 5614 cm^{-1}, respectively; Figure 6). Complexation induces a
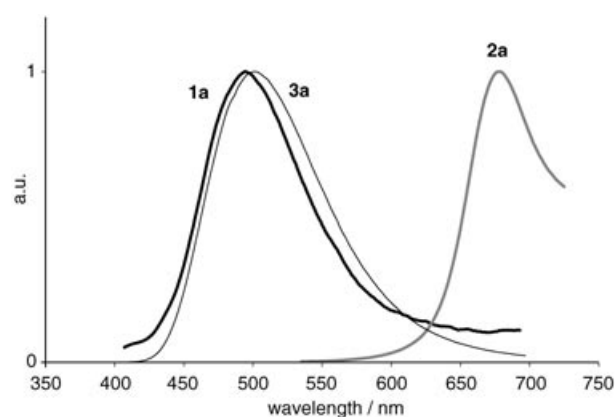

Figure 6. Fluorescence spectra of complexes **1a** (bold), **2a** (gray) and **3a** (black).

significant red shift of the emission wavelength when compared to that of free ligands ($\Delta\lambda_{em}$(complex vs ligand) = 90 and 147 nm for **1a/a** and **1b/b**, respectively), and, as expected, the λ_{em} values decrease with the relative Lewis acidity in the order Zn$^{2+}\approx$Fe$^{2+}>$Hg$^{2+}\gg$Ag$^+$ (Table 1). In contrast, upon excitation at the MLCT or the ILCT wavelength, ruthenium complexes **2a** and **2b** feature a red-shifted photoluminescence at 678 and 721 nm, respectively (Table 1 and Figure 6). Their excitation spectra overlay the absorption spectra with two maxima corresponding to the ILCT and MLCT transitions, indicating that the observed emission arise from MLCT triplet states.[18h] The room-temperature solution emission spectrum of Cu^{I} **5b′** is also very different to that of Ag^{I} **6b′**; whereas **6b′** exhibits a broad ILCT luminescence at 562 nm, **5b′** shows a weak, red-shifted, MLCT emission at 621 nm, similar to that of **5b′**·4H$^+$.

Nonlinear optical properties: The harmonic light scattering (HLS) technique was used for the molecular hyperpolarizability (β) measurements.[34] It is also well-known that two-photon-induced fluorescence may significantly affect HLS measurements leading to an important overestimation of the

hyperpolarizability values.[35] Initial measurements with $\lambda = 1.34\,\mu m$ as the fundamental wavelength confirmed the importance of the multiphoton fluorescence contribution. New β measurements that used $\lambda = 1.91\,\mu m$ as the fundamental wavelength were performed, because the second harmonic wavelength at 955 nm is far from the possible two-photon resonance, thus making any contribution from two-photon absorption-induced fluorescence to the HLS signal negligible. For example, $\beta^{1.91} = 340 \times 10^{-30}$ esu for **1b** is far below the $\beta^{1.34}$ value of 940×10^{-30} esu. Similar behavior was observed for complexes **2a**, **2b**, and **3b**, indicating that the two-photon-induced fluorescence is a general phenomenon for the whole family of tris(bipyridyl) metal complexes (Table 1). In contrast, the more "transparent" tetrahedral Cu^I **5b′** exhibited a similar β_0 value calculated from $\beta^{1.34}$ and $\beta^{1.91}$ values.

As usually observed by experimental measurements[4k,m,5a] and predicted by theoretical calculations,[36] the dispersion-free hyperpolarizability coefficient of octupolar chromophores monotonically increases with an increase of the ground state charge-transfer character. This can be achieved either by increasing the donor strength of the substituent or by tuning the π-conjugated system. Indeed, replacing the octyloxy group (**1a**) by a stronger dibutylamino donor group (**1b**) results in a 20% enhancement of β_0, from 200 to 240×10^{-30} esu.[37] In addition, changing the phenyl ring of the styryl moieties (**1b**) for a thienyl ring (**1c**) leads to a 10% enhancement of β_0. Such enhancement, already observed in dipolar NLO,[38] can be explained by 1) the lower aromatic stabilization energy of the thienyl versus the phenyl fragment (28 vs 36 kcal mol^{-1}),[39] which induces improved delocalization and 2) the auxiliary donor ability of the electron-rich thienyl ring, which increases the intramolecular charge-transfer character.[40] On the other hand, replacing the C=C bond of the styryl moieties (**1b**) by a C=N bond (**1c**) results in a significant decrease of β_0, despite the important bathochromic shift of the ILCT transition ($\Delta\lambda = 33$ nm). These apparently antagonistic effects have already been observed for dipolar NLO-phores,[41] and are not fully rationalized. According to theoretical calculations,[42] the bathochromic shift of the ILCT transition seems to be caused by the higher electronegativity of the nitrogen atom, as compared to carbon, which induces a supplementary dipole moment. On the other hand, the presence of the nitrogen atom in the π-conjugated system can contribute to the localization of the charge, hence to a decrease in the NLO activity. Finally, by lengthening the conjugation bridge, such as in **1e** featuring two styryl moieties (Figure 7), a 2.7 times enhancement of β_0 is achieved (β_0(**1e**) = 657×10^{-30} esu vs. β_0(**1b**) = 241×10^{-30} esu). Similar enhancement upon increasing the π-conjugated backbone have always been observed in the literature. Indeed Cho et al.[4m] and Blanchard-Desce et al.[41] reported a 1.5× and 5.5× enhancement, respectively, of the β_0 value upon incorporating a styryl moiety into D_3 symmetric octupolar compounds. To the best of our knowledge, the β_0 value of **1e** is the largest ever reported for an octupolar molecule. Thus, this study shows that the nature of the bipyridyl ligand has a strong influence on the NLO activity of the corresponding trisbipyridyl zinc complexes. However, it
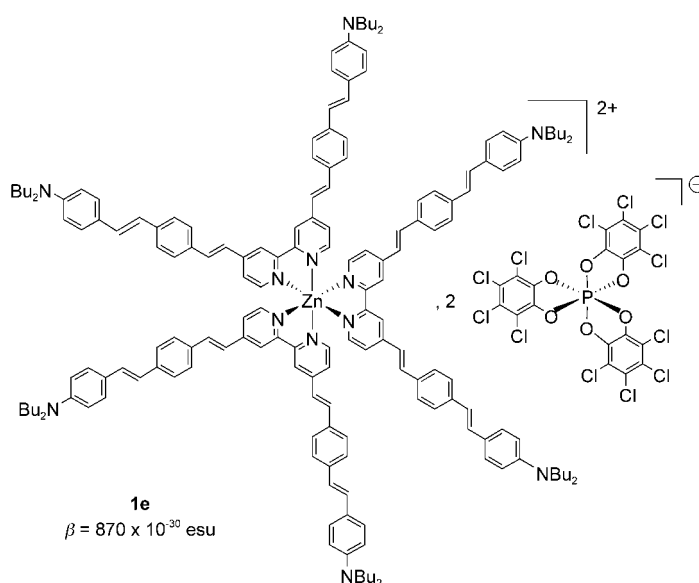

Figure 7. Chemical structure of **1e** displaying the highest NLO activity.

is clearly that the elongation of the π-conjugated backbone is the key parameter to maximize the NLO activity. The strength of the donor group or the nature of the transmitter has a strong influence on the optical properties, but only a weaker influence on the NLO properties.

As described previously, the influence of the central metal on the linear optical data—particularly the red shift of the ILCT transition—can be correlated to the Lewis acidity of the metallic ion. For example, this is clearly shown in the D_{2d} symmetric $[M(\mathbf{b'})_2]^{n+}$ series ($M^{n+} = Cu^+$, Ag^+, and Zn^{2+}), whereby the ILCT transitions show roughly the same oscillator strength,[43] but with a pronounced bathochromic shift for Zn^{2+} versus Cu^+ and Ag^+. The β_0 value is also strongly correlated with the metal Lewis acidity, since that of $[Zn(\mathbf{b'})_2]^{2+}$ is about twice that of the corresponding copper and silver compounds (157 vs. 86 and 70×10^{-30} esu, respectively). This result underlines the importance of the metallic core not only as a template to gather ligands in a predetermined octupolar arrangement, but also for its direct participation in the ground-state charge transfer and NLO activity. Another important aspect of the role of central metal ion is given by the peculiar case of zinc(II), which has the ability to expand its coordination sphere, since there is no ligand field stabilization effect, and, therefore, can give tetrahedral and octahedral complexes with bipyridine ligands. Thus, this characteristic provided a unique opportunity to design either dipolar $[Zn(\mathbf{b})Cl_2]$ or octupolar D_{2d} $[Zn(\mathbf{b'})_2][OTf]_2$ and D_3 $[Zn(\mathbf{b})_3][PF_6]_2$ molecules by simple controlled combination of one, two, or three bipyridyl ligands with zinc(II) (Figure 8).[18f] These complexes are intense dyes that exhibit high molecular extinction coefficients, and the oscillator strength[43] follows a 1:1.8:2.9 ratio (theoretical = 1:2:3) ratio for $[Zn(\mathbf{b})Cl_2]$, **1b′**, and **1b**, respectively, as expected for non-interacting subchromophores.[4f,8b] Importantly, the β_0 values (Table 1) follow the same tendency and monotonically increase from dipolar to D_3 octupolar compounds with respect to the number of sub-
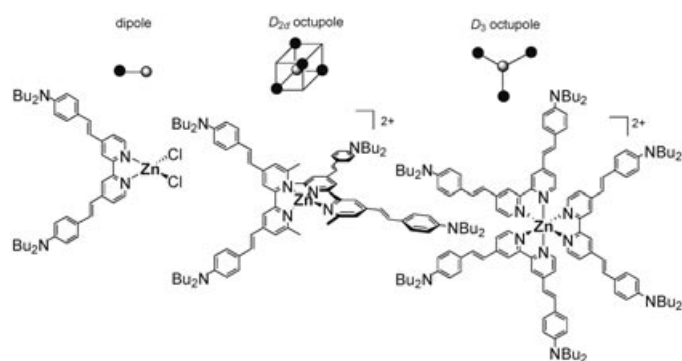
Figure 8. Dipolar and octupolar architectures based on zinc(II) complexes.

chromophores organized around the Zn^{II} center. An improved transparency/nonlinearity trade-off is reached for the octahedral complex **1b**, as compared to the tetrahedral complex **1b′**. These results also point out the efficiency of the octupolar strategy, since **1b** exhibits a β_0 value that is roughly four times larger than that of the corresponding dipolar derivative, but without the undesirable bathochromic shift of the ILCT transition ($\Delta\lambda = 14$ nm). Thus, this is a nice illustration of the superiority of octupoles versus dipoles in terms of nonlinearity without significant cost of transparency.

Role of the MLCT transition with regard to NLO activity: In addition to the ILCT transition, ruthenium and iron complexes **2a,b** and **3a,b**, each show an MLCT band in the visible region that also contributes to the NLO activity. Therefore, we sought to estimate the influence of both transitions to the total the molecular hyperpolarizability. In a first approximation, these ILCT and MLCT are roughly parallel but in opposite direction. Electroabsorption (Stark) spectroscopy was recently used by Vance and Hupp to calculate the contributions from both MLCT and ILCT transitions to the NLO response on an octupolar ruthenium complex similar to **2b**.[30] They suggested that the total hyperpolarizability (β_{TOT}) results from the summation of the two contributions β_{ILCT} and β_{MLCT} that are in opposite sign and thus destructively interfere [Eq. (1)].

$$\beta_{TOT} = |\beta_{ILCT}| - |\beta_{MLCT}| \qquad (1)$$

As the λ_{ILCT} values of the Ru^{II}, Zn^{II}, and Fe^{II} complexes are roughly similar, one can anticipate that, according to Equation (1), $\beta(Zn) > \beta(Ru) > \beta(Fe)$, because Zn^{II} complexes do not display any MLCT and that of Fe^{II} is red-shifted compared to that of Ru^{II}. Experimental measurements (Table 1) clearly show that $\beta(Zn) > \beta(Fe)$; however, the β values of Ru^{II} complexes **2a,b** are as large as those of the corresponding Zn^{II} complexes **1a** and **1b**, despite the presence of an MLCT transition ($\beta(\mathbf{1b}) = \beta(\mathbf{2b}) = 340 \times 10^{-30}$ esu, $\beta(\mathbf{1a}) = 250 \times 10^{-30}$ esu, and $\beta(\mathbf{2a}) = 270 \times 10^{-30}$ esu). Thus, the proposed model based on an antagonist contribution of both ILCT and MLCT does not allow rationalization of all the experimental results.

Conclusion

In conclusion, this study shows that coordination chemistry is a very useful tool for the design of either tetrahedral or octahedral octupolar NLO-phores. The molecular quadratic hyperpolarizability (β) values are strongly influenced by the symmetry of the complexes, the nature of the ligands, and the nature of the metallic centers. A careful examination of the NLO measurements allows us to draw some general conclusions:

1) With regard to the ligand: the length of the π-conjugated backbone clearly appears to have a stronger influence on β than the strength of the donor group.
2) With regard to the metal ion: the increase of its Lewis acidity results in a significant enhancement of the NLO activity.
3) An increase of the coordination number, thus an increase of ligand-to-metal ratio, also results in a substantial enhancement of β.
4) The contribution of the MLCT transition to the molecular hyperpolarizability still remains unclear.

Finally this study opens new perspectives for the optimization of the molecular quadratic hyperpolarizability of coordination complexes by switching from transition metals to *f* elements such as lanthanides(III), which are well-known for their strong Lewis acidity and their ability to accept large coordinance. Further studies are currently being developed in our laboratory.

Experimental Section

General procedures: All reactions were routinely performed under argon with Schlenk techniques. NMR spectra (^1H, ^{13}C, ^{31}P) were recorded at room temperature on BRUKER DPX 200, AC 300, or DMX 500 spectrometers operating at 200.12, 300.13, and 500.13 MHz, respectively, for ^1H. NMR data are reported relative to tetramethylsilane (^1H, ^{13}C), residual solvent peaks being used as the internal standard (CD_2Cl_2; $\delta = 5.25$ ppm (^1H), $\delta = 53.45$ ppm (^{13}C)). Complete assignment of the ^1H and ^{13}C spectra required 2D experiments (COSY, NOESY, H–C correlation (hmqc and hmbc sequences)). The classical atom numbering scheme for bipyridyl-based complexes is depicted in Figure 9. UV-visible spectra were recorded on a KONTRON UVIKON 941 spectrophotometer in dilute dichloromethane solution ($\approx 10^{-5}$ mol L^{-1}). Fluorescence experiments were performed in dilute dichloromethane solution ($\approx 10^{-5}$ mol L^{-1}) with a PTI spectrometer. Thermal stability was measured by means of a TA instrument TGA 2050 Thermogravimetric Analyzer. The decomposition temperature at 5 and 10 % weight lost are designated
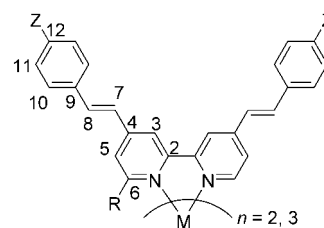

Figure 9. Generic atom numbering of the functionalized-bipyridyl ligands and related complexes. The labels are used for the assignment of the ^1H and ^{13}C NMR signals.

Td$_5$ and Td$_{10}$, respectively. The heating program used was: 1) isothermal at 50 °C for 15 min, 2) a temperature ramp of 10 °C min^{-1} up to 600 °C. High-resolution mass spectrometry measurements (FAB) were performed at the Centre Regional de Mesures Physiques de L'Ouest (Rennes, France) and elemental analysis by the Service Central d'Analyse du CNRS (Solaize, France).

Chemicals: The bipyridyl ligands 4,4′-bis(octyloxystyryl)-2,2′-bipyridine (**a**), 4,4′-bis(dibutylaminostyryl)-2,2′-bipyridine (**b**), 4,4′-bis(dibutylamino-thienylvinyl)-2,2′-bipyridine (**c**), and 4,4′-diformyl-2,2′-bipyridine were synthesized following reported procedures.[19] N,N-Dibutyl-1,4-phenylenediamine was synthesized by Zn/HCl reduction of the p-nitrosodibutylaniline precursor (86 % yield), and distilled under vacuum (130 °C/0.1 bar) before use. 4,4′,6,6′-Tetramethyl-2,2′-bipyridine was synthesized on 10 g scale by means of Na coupling of lutidine and purified by sublimation. N,N-Dibutylanimobenzaldehyde and N-methyl-N-octylaminobenzaldehyde were classically prepared by a Vilsmeier–Haack formylation. [HNBu$_3$][TRISPHAT] was obtained on a 10 g scale, as described in the literature.[22a] [Cu(CH$_3$CN)$_4$][PF$_6$] and [RuCl$_2$(dmso)$_4$] were synthesized according to published procedures.[44] Other metallic salts are commercially available and were used without purification. THF was distilled over Na/benzophenone, DMF was distilled prior use, and CH$_2$Cl$_2$ was distilled over CaH$_2$.

Harmonic light scattering (HLS) measurements: The 1.91 µm fundamental beam was emitted by a high-pressure (30 bar), 50 cm long Raman cell pumped by a Nd^{3+}:YAG laser operating at 1.06 µm (or 1.34 µm) with a 10 Hz repetition rate and pulses of 15 ns duration. Only the back-scattered 1.91 µm Raman emission was collected at a 45° incidence angle by use of a dichroic mirror in order to eliminate most of the residual 1.06 µm pump photons. Our reference sample was a concentrated (10^{-2} mol L^{-1}) solution of ethyl violet, its octupolar $\beta = \beta_{(J=3)}$ value being calibrated at 1.91 µm with respect to that of the N-4-nitrophenyl-prolinol (NPP) reference dipolar molecule, leading to $\beta = 170 \times 10^{-30}$ esu for ethyl violet at 1.91 µm. It must be noted that most classical organic solvents are not transparent at 1.91 µm, although chlorinated solvents are an exception, hence the use of dichloromethane for the HLS measurements. The HLS photons at 955 nm were focused onto the photomultiplier tube by two collecting lenses (we used a Hamamatsu R632–01 photomultiplier tube). The detected signal was then sampled and averaged by a boxcar, and processed by a computer. The reference beam was collected at a 45° incidence angle by a glass plate, and focused onto a highly nonlinear NPP powder, which was used as the frequency doubler.[45] The variation of the scattered second harmonic intensity from the solution was recorded on the computer as a function of the reference second harmonic signal provided by the NPP powder, which scales as the square of the incoming fundamental intensity. Values for β were then inferred from the slopes of the resulting lines.

4,4′-Bis(dibutylaminophenylimino)-2,2′-bipyridine (d): 4,4′-Diformyl-2,2′-bipyridine (219 mg, 1.03 mmol) was dissolved in CH$_2$Cl$_2$ (10 mL). Freshly distilled N,N-dibutyl-1,4-phenylene diamine (500 mg, 2.27 mmol) was added, and the mixture was stirred for 2 h. The green-yellow reaction mixture was filtered, and the solvent was evaporated. The resulting solid was dissolved in CH$_2$Cl$_2$ and purified by precipitation with pentane (v/v = 1:10) to yield **d** as a green-yellow powder (550 mg, 85 %). ^{1}H NMR (CDCl$_3$): $\delta = 8.75$ (d, ^3J(H,H) = 5 Hz, 2H; H6), 8.70 (br s, 2H; H7), 8.60 (s, 2H; H3), 7.87 (d, ^3J(H,H) = 5 Hz, 2H; H5), 7.30 (d, ^3J(H,H) = 9.0 Hz, 4H; H10), 6.62 (d, ^3J(H,H) = 9.0 Hz, 4H; H11), 3.30 (t, ^3J(H,H) = 8.0 Hz, 8H; H13), 1.51 (m, 8H; H14), 1.35 (m, 8H; H15), 0.96 ppm (t, ^3J(H,H) = 7.0 Hz, 12H; H16); ^{13}C NMR (CDCl$_3$): $\delta = 157.0$ (C2), 151.3 (C7), 149.7 (C6), 148.2 (C12), 145.2 (C4), 138.1 (C9), 123.3 (C11), 121.1 (C5), 120.6 (C3), 111.8 (C10), 51.0 (C13), 29.5 (C14), 20.4 (C15), 14.1 ppm (C16); UV/Vis (CH$_2$Cl$_2$): λ_{max} (ε) = 436 nm (39 000 L mol^{-1} cm^{-1}); TGA: Td$_5$ = 205 °C, Td$_{10}$ = 255 °C; HRMS (FAB): calcd for C$_{40}$H$_{53}$N$_6$ [M+H]$^+$: 617.4332; found: 617.4329.

4,4′-Bis(diethylphosphonomethyl)-2,2′-bipyridine:[46] A solution of 4,4′-bis-bromomethyl-2,2′-bipyridine (630 mg, 1.8 mmol) and triethylphosphite (5 mL, 0.29 mol) in chloroform (5 mL) was refluxed for 3 h. The solution was then allowed to cool to room temperature, and chloroform and triethylphosphite were removed under reduced pressure. The oily brown residue was taken up with pentane (20 mL), resulting in the precipitation of the desired product. The pale brown solid was washed with pentane (2×20 mL) and dried under reduced pressure (730 mg, 93 %).

^{1}H NMR (CDCl$_3$, 200 MHz): $\delta = 8.58$ (d, ^3J(H,H) = 4.9 Hz, 2H; H6), 8.32 (s, 2H; H3), 7.31–7.29 (m, 2H; H5), 4.05 (dq, ^3J(P,H) = 7 Hz, 8H; ^3J(H,H) = 7 Hz, H8) 3.22 (d, 4H; ^2J(P,H) = 22.2 Hz, H7), 1.25 ppm (t, 12H; ^3J(H,H) = 7 Hz, H9°); ^{31}P NMR (CDCl$_3$, 81 MHz): $\delta = 25.64$ ppm.

4,4′-Bis(dibutylaminostyrylstyryl)-2,2′-bipyridine (e): Potassium terbutoxide (486 mg, 4.3 mmol) was added to a solution of [N,N-(dibutylamino)-styryl]benzaldehyde (1.27 g, 3.8 mmol) and 4,4′-bis(diethylphosphonomethyl)-2,2′-bipyridine (730 mg, 1.7 mmol) in THF (30 mL). The reaction mixture was stirred for 2 h at room temperature. After addition of water (10 mL), THF was removed under reduced pressure, and the aqueous residue was extracted with CH$_2$Cl$_2$ (3×30 mL). The collected organic layers were washed with brine (30 mL) and water (50 mL), dried over magnesium sulfate, and filtered. After evaporation of the solvent, precipitation from CH$_2$Cl$_2$/pentane (v/v = 1:10), and further recrystallization in ethyl acetate, the product was obtained as an orange powder (1.1 mg, 76 %). ^{1}H NMR (500.13 MHz, CD$_2$Cl$_2$): $\delta = 8.69$ (d, ^3J(H,H) = 4.9 Hz, 2H; H6), 8.63 (s, 2H; H3), 7.61 (d, ^3J(H,H) = 8.2 Hz, 4H; H10), 7.55 (d, ^3J(H,H) = 8.2 Hz, 4H; H11), 7.51 (d, ^3J(H,H) = 16.3 Hz, 2H; H8), 7.47 (d, ^3J(H,H) = 4.9 Hz, 2H; H5), 7.42 (d, ^3J(H,H) = 8.7 Hz, 4H; H16), 7.21 (d, ^3J(H,H) = 16.3 Hz, 2H; H7), 7.14 (d, ^3J(H,H) = 16.2 Hz, 2H; H14), 6.94 (d, ^3J(H,H) = 16.2 Hz, 2H; H13), 6.68 (d, ^3J(H,H) = 8.7 Hz, 4H; H17), 3.35 (t, ^3J(H,H) = 7.5 Hz, 8H; H19), 3.36 (q, ^3J(H,H) = 7.5 Hz, 8H; H20), 1.41 (st, ^3J(H,H) = 7.5 Hz, 8H; H21), 1.01 ppm (t, ^3J(H,H) = 7.5 Hz, 12H; H22); ^{13}C NMR (125.77 MHz, CD$_2$Cl$_2$): $\delta = 156.5$ (C2), 149.5 (C6), 148.1 (C18), 145.7 (C4), 138.9 (C12), 134.6 (C9), 132.8 (C8), 129.6 (C14), 127.8 (C16), 127.4 (C10), 126.2 (C11), 125.3 (C7), 124.1 (C15), 122.5 (C13), 120.8 (C5), 117.9 (C3), 111.6 (C17), 50.7 (C19), 29.4 (C20), 20.3 (C21), 13.8 ppm (C22); UV/Vis (CH$_2$Cl$_2$): λ_{max} (ε) = 420 nm (78 000 L mol^{-1} cm^{-1}); emission (CH$_2$Cl$_2$): λ_{em} = 598 nm; TGA: Td$_{5-10}$ = 330–360 °C; HRMS (FAB): calcd for C$_{58}$H$_{67}$N$_4$ [M+H]$^+$: 819.5366; found: 819.5364; elemental analysis calcd (%) for C$_{58}$H$_{66}$N$_4$·CH$_2$Cl$_2$: C 78.38, H 7.58, N 6.20; found: C 79.09, H 7.76, N 6.08.

General procedure for the preparation of tris(bipyridyl)zinc complexes: Zn(OAc)$_2$·2H$_2$O and the corresponding bipyridyl ligand (3 equiv) were dissolved in ethanol (30 mL). The mixture was heated under reflux for 15 h. The solution was then cooled to room temperature, and an aqueous solution of NaPF$_6$ (6 equiv, 20 mL) was added. The resulting precipitate was filtered off, dissolved in CH$_2$Cl$_2$, and dried with MgSO$_4$. After filtration and evaporation of the solvent, the solid was purified further by precipitating several times with CH$_2$Cl$_2$/pentane (v/v = 1:10). The solvents were removed under vacuum to afford the desired product as a microcrystalline powder.

[Zn(b)$_3$][PF$_6$]$_2$ (1b): Orange powder, 83 % yield; ^{1}H NMR (CD$_2$Cl$_2$) ^{1}H NMR: $\delta = 8.37$ (s, 6H; H3), 7.77 (d, ^3J(H,H) = 5.6 Hz, 6H; H6), 7.49 (d, ^3J(H,H) = 16.1 Hz, 6H; H8), 7.48 (d, ^3J(H,H) = 5.6 Hz, 6H; H5), 7.47 (d, ^3J(H,H) = 8.9 Hz, 12H; H10), 6.95 (d, ^3J(H,H) = 16.1 Hz, 6H; H7), 6.64 (d, ^3J(H,H) = 8.9 Hz, 12H; H11), 3.31 (t, ^3J(H,H) = 7.3 Hz, 24H; H13), 1.57 (m, 24H; H14), 1.34 (m, 24H; H15), 0.94 ppm (t, ^3J(H,H) = 7.3 Hz, 36H; H16); ^{13}C NMR (CD$_2$Cl$_2$): $\delta = 151.3$ (C2), 149.8 and 149.7 (C12 or C4), 147.0 (C6), 138.0 (C8), 129.5 (C10), 122.3 (C5), 122.0 (C9), 119.5 (C3), 117.6 (C7), 111.5 (C11), 50.7 (C13), 29.4 (C14), 20.3 (C15), 13.7 ppm (C16); UV/Vis (CH$_2$Cl$_2$): λ_{max} (ε) = 466 nm (175 000 L mol^{-1} cm^{-1}); TGA: Td$_5$ = 285 °C, Td$_{10}$ = 330 °C; HRMS (only fragmentation peaks were observed): calcd for C$_{84}$H$_{108}$N$_8$FZn [Zn(b)$_2$F]$^+$: 1311.7972; found: 1311.8043; LRMS: calcd for C$_{42}$H$_{54}$N$_4$FZn [Zn(b)F]$^+$: 697.4; found: 697.4; elemental analysis calcd (%) for C$_{126}$H$_{162}$N$_{12}$P$_2$F$_{12}$Zn: C 68.81, H 7.42, N 7.64; found: C 69.02, H 7.24, N 7.41.

[Zn(c)$_3$][PF$_6$]$_2$ (1c): Dark-red powder, 73 % yield; ^{1}H NMR (CD$_2$Cl$_2$): $\delta = 9.02$ (s, 6H; H7), 8.69 (s, 6H; H3), 7.95 (d, ^3J(H,H) = 11 Hz, 6H; H6), 7.42 (d, ^3J(H,H) = 8.0 Hz, 12H; H10), 6.66 (d, ^3J(H,H) = 8.0 Hz, 12H; H11), 3.31 (t, ^3J(H,H) = 8.0 Hz, 24H; H13), 1.57 (m, 24H; H14), 1.34 (m, 24H; H15), 0.94 ppm (t, ^3J(H,H) = 7.2 Hz, 36H; H16); ^{13}C NMR (CD$_2$Cl$_2$): $\delta = 149.6$ (C2, C4), 149.3 (C12), 148.0 (C6), 146.6 (C7), 136.6 (C9), 125.3 (C5), 124.3 (C10), 120.8 (C3), 111.7 (C11), 50.9 (C13), 29.4 (C14), 20.3 (C15), 13.7 ppm (C16); UV/Vis (CH$_2$Cl$_2$): λ_{max} = 506 nm (68 000 L mol^{-1} cm^{-1}); LRMS (only fragmentation peaks were observed): calcd for C$_{80}$H$_{104}$N$_{12}$FZn [Zn(c)$_2$F]$^+$: 1315.7; found: 1315.9; calcd for C$_{40}$H$_{52}$N$_6$FZn [Zn(c)F]$^+$: 699.4; found: 699.4.

[Zn(d)$_3$][PF$_6$]$_2$ (1d): Dark-red powder, 84 % yield; ^{1}H NMR (CD$_2$Cl$_2$): $\delta = 8.11$ (s, 6H; H3), 7.63 (d, ^3J(H,H) = 5.5 Hz, 6H; H6), 7.55 (d,

$^3J(H,H) = 15.5$ Hz, 6H; H8), 7.26 (d, $^3J(H,H) = 5.5$, 6H; H5), 7.01 (d, $^3J(H,H) = 4.1$ Hz, 6H; H10), 6.32 (d, $^3J(H,H) = 15.5$ Hz, 6H; H7), 5.77 (d, $^3J(H,H) = 4.1$ Hz, 6H; H11), 3.29 (t, $^3J(H,H) = 7.3$ Hz, 24H; H13), 1.58 (m, 24H; H14), 1.28 (m, 24H; H15), 0.93 ppm (t, $^3J(H,H) = 7.3$ Hz, 36H; H16); ^{13}C NMR(CD$_2$Cl$_2$): $\delta = 161.3$ (C12), 151.0 (C4), 149.6 (C2), 146.8 (C6), 139.5 (C10), 131.5 (C8), 122.9 (C9), 121.4 (C5), 117.7 (C3), 114.1 (C7), 101.8 (C11), 53.6 (C13), 29.2 (C14), 20.2 (C15), 13.7 ppm (C16); UV/Vis (CH$_2$Cl$_2$): λ_{max} (ε) = 519 nm (50 000 L mol^{-1} cm^{-1}); LRMS (only fragmentation peaks were observed): calcd for C$_{76}$H$_{100}$N$_8$FS$_4$Zn [Zn(**d**)$_2$F]$^+$: 1335.6; found: 1335.7; calcd for C$_{38}$H$_{50}$N$_4$FS$_2$Zn [Zn(**d**)F]$^+$: 709.3; found: 709.3.

[Zn(a)$_3$][TRISPHAT] (1a): Unclean [Zn(**a**)$_3$][PF$_6$]$_2$ (290 mg, 0.13 mmol), resulting from the reaction between Zn(OAc)$_2\cdot$2H$_2$O and **a** (3 equiv) in refluxing methanol followed by an anion exchange with NaPF$_6$, was dissolved in CH$_2$Cl$_2$ (20 mL) in a round-bottom flask. [HNBu$_3$][TRISPHAT] (251 mg, 0.26 mmol) was added, and the yellow solution was stirred for 2 h. The solvent was evaporated, and the product was filtered through a column of silica gel (eluent: CH$_2$Cl$_2$). After evaporation of the solvent under vacuum and recrystallization from CH$_2$Cl$_2$/pentane (v/v = 1:10), the product was recovered as a yellow powder (266 mg, 58 %). ^{1}H NMR (CD$_2$Cl$_2$): $\delta = 8.65$ (d, $^3J(H,H) = 5$ Hz, 6H; H6), 8.41 (s, 6H; H3), 7.40 (d, $^3J(H,H) = 8.9$ Hz, 12H; H10), 7.22 (d, $^3J(H,H) = 5$ Hz, 6H; H5), 7.13 (d, $^3J(H,H) = 16.1$ Hz, 6H; H8), 6.89 (d, $^3J(H,H) = 8.9$ Hz, 12H; H11) 6.71 (d, $^3J(H,H) = 16.1$ Hz, 6H; H7), 6.91, 3.97 (t, $^3J(H,H) = 6.5$ Hz, 12H; H13), 1.75 (m, 12H; H14), 1.5–1.2 (m, 60H; H15–19), 0.86 ppm (t, $^3J(H,H) = 6.5$ Hz, 18H; H20); ^{13}C NMR (CD$_2$Cl$_2$): $\delta = 161.2$ (C4), 150.6 (C2), 149.8 (C6), 149.7 (C12), 141.9 (d, $J(C,P) = 6$ Hz; TRISPHAT), 136.7 (C8), 129.7 (C10), 128.4 (C9), 123.2 (TRISPHAT), 123.1 (C7), 121.1 and 119.7 (C3 or C5), 115.2 (C11), 114.6 (d, $J(C,P) = 19$ Hz; TRISPHAT), 68.7 (C13), 32.3 (C14), 29.8 (C15), 29.7 (C16), 29.6 (C17), 26.5 (C18), 23.1 (C19), 14.4 ppm (C20); ^{31}P NMR (CD$_2$Cl$_2$): $\delta = -79.5$ ppm; UV/Vis (CH$_2$Cl$_2$): λ_{max} (ε) = 382 nm (128 000 L mol^{-1} cm^{-1}); emission (CH$_2$Cl$_2$): λ_{em} = 501 nm; TGA: Td$_5$ = 330 °C, Td$_{10}$ = 335 °C; elemental analysis calcd (%) for C$_{162}$H$_{15}$N$_6$O$_{18}$Cl$_{24}$P$_2$Zn: C 55.93, H 4.52, N 2.42, found: C 55.94, H 4.64, N 2.38.

[Zn(e)$_3$][TRISPHAT]$_2$ (1e): Zn(OAc)$_2\cdot$2H$_2$O (45 mg, 0.2 mmol) and ligand **e** (0.5 g, 0.6 mmol) were dissolved in ethanol (20 mL). The mixture was heated under reflux for 15 h. The solution was then cooled to room temperature, and [HNBu$_3$][TRISPHAT] (389 mg, 0.4 mmol) was added. The orange solution was stirred for 2 h and then poured into water (150 mL). The resulting red precipitate was filtered, dissolved in CH$_2$Cl$_2$, and dried with MgSO$_4$. After filtration and evaporation of the solvent, the solid was purified further by precipitating it several times from CH$_2$Cl$_2$/pentane (v/v = 1:10). The solvents were removed under vacuum to afford the desired product as a microcrystalline powder (0.6 g, 73 %). ^{1}H NMR (500.13 MHz, CD$_2$Cl$_2$): $\delta = 8.74$ (d, $^3J(H,H) = 5.4$ Hz, 6H; H6), 8.49 (s, 6H; H3), 7.42–7.38 (m, 24H; H10 and H11), 7.32 (d, $^3J(H,H) = 8.5$ Hz, 12H; H16), 7.31 (d, $^3J(H,H) = 5.8$ Hz, 6H; H5), 7.26 (d, $^3J(H,H) = 16.2$ Hz, 6H; H8), 7.16 (d, $^3J(H,H) = 16.2$ Hz, 6H; H14), 6.89 (d, $^3J(H,H) = 16.2$ Hz, 12H; H7 and H13), 6.64 (d, $^3J(H,H) = 8.6$ Hz, 12H; H17), 3.31 (t, $^3J(H,H) = 7.2$ Hz, 24H; H19), 1.61–1.58 (m, 24H; H20), 1.37 (st, $^3J(H,H) = 7.2$ Hz, 24H; H21), 0.96 ppm (t, $J = 7.5$ Hz, 36H; H22); ^{13}C NMR (125.77 MHz, CD$_2$Cl$_2$): $\delta = 150.4$ (C2), 149.8 (C6), 148.7 (C18), 142.0 (d, $J(C,P) = 6$ Hz; TRISPHAT), 140.6 (C4), 136.8 (C8), 133.6 (C12), 130.7 (C14), 128.6 (C16, C9), 128.4 (C10), 126.6 (C11), 124.3 (C15), 123.4 (C7 TRISPHAT), 122.8 (C13), 122.5 (C5), 119.9 (C3), 114.6 (d, $J(C,P) = 19.9$ Hz; TRISPHAT), 112.0 (C17), 51.1 (C19), 29.8 (C20), 20.7 (C21), 14.2 ppm (C22); ^{31}P NMR (121.49 MHz, CD$_2$Cl$_2$): $\delta = -80.57$ ppm; UV/Vis (CH$_2$Cl$_2$): λ_{max} (ε) = 482 nm (132 000 L mol^{-1} cm^{-1}); TGA: Td$_{10}$ = 285 °C; elemental analysis calcd (%) for C$_{210}$H$_{198}$N$_{12}$O$_{12}$Cl$_{24}$P$_2$Zn$\cdot$CH$_2$Cl$_2$: C 61.14, H 4.86, N 4.05; found: C 61.22, H 4.98, N 3.83.

[Ru(a)$_3$][PF$_6$]$_2$: Ruthenium trichloride hydrate (130 mg, 0.5 mmol) and ligand **a** (3 equiv) were dissolved in dry DMF (20 mL). The mixture was heated at reflux under nitrogen for 7 h, and the solution was allowed to cool to room temperature. A solution of NaPF$_6$ (0.2 g, 1.2 mmol) in water (20 mL) was added to afford a dark brown precipitate. The crude product was dissolved in CH$_2$Cl$_2$ and washed with water. The organic layer was dried with MgSO$_4$ and concentrated by evaporation, and the product was precipitated by addition of pentane (v/v = 1:10). Finally, the red microcrystalline powder (95 %) was dried under vacuum. ^{1}H NMR

(CDCl$_3$): $\delta = 8.54$ (d, $^4J(H,H) = 1.5$ Hz, 6H; H3), 7.62 (d, $^3J(H,H) = 6.1$ Hz, 6H; H6), 7.58 (d, $^3J(H,H) = 8.8$ Hz, 12H; H10), 7.50 (d, $^3J(H,H) = 16.3$ Hz, 6H; H8), 7.45 (dd, $^3J(H,H) = 6.1$ $^4J(H,H) = 1.5$ Hz, 6H; H5), 7.10 (d, $^3J(H,H) = 16.3$ Hz, 6H; H7), 6.91 (d, $^3J(H,H) = 8.8$ Hz, 12H; H11), 3.96 (t, $^3J(H,H) = 6.5$ Hz, 12H; H13), 1.74 (m, 12H; H14), 1.27 (m, 60H; H15–19), 0.86 ppm (t, $^3J(H,H) = 6.0$ Hz, 18H; H20); ^{13}C NMR (CD$_2$Cl$_2$): $\delta = 160.7$ (C4), 157.0 (C2), 150.4 (C6), 147.3 (C12), 136.6 (C8), 129.2 (C10), 122.9 (C9), 123.6 (C7), 121.1 and 120.9 (C3 or C5), 114.9 (C11), 68.2 (C13), 31.8 (C14), 29.3 (C15), 29.2 (C16), 29.1 (C17), 26.0 (C18), 22.7 (C19), 13.9 ppm (C20); UV/Vis (CH$_2$Cl$_2$): λ_{max} (ε) = 387 nm (125 000 L mol^{-1} cm^{-1}); λ_{MLCT} (ε) = 482 nm (41 000 L mol^{-1} cm^{-1}); elemental analysis calcd (%) for C$_{126}$H$_{15}$N$_6$O$_6$P$_2$F$_{12}$Ru$\cdot$CH$_2$Cl$_2$: C 65.56, H 6.85, N 3.61; found: C 65.05, H 7.00, N 3.57.

[Ru(b)$_3$][PF$_6$]$_2$ (2b): This complex was prepared following the same procedure as for **2a**, but from bipyridyl ligand **b**. Yield: 96 %; ^{1}H NMR (CD$_2$Cl$_2$): $\delta = 8.41$ (br s, 6H; H3), 7.56 (d, $^3J(H,H) = 6$ Hz, 6H; H6), 7.48 (d, $^3J(H,H) = 8.9$ Hz, 12H; H10), 7.47 (d, $^3J(H,H) = 16.0$ Hz, 6H; H8), 7.36 (d, $^3J(H,H) = 6$ Hz, 6H; H5), 6.96 (d, $^3J(H,H) = 16$ Hz, 6H; H7), 6.65 (d, $^3J(H,H) = 9$ Hz, 12H; H11), 3.31 (t, $^3J(H,H) = 7.4$ Hz, 24H; H13), 1.57 (m, 24H; H14), 1.35 (m, 24H; H15), 0.95 ppm (t, $^3J(H,H) = 7.3$ Hz, 36H; H16); ^{13}C NMR (CD$_2$Cl$_2$): $\delta = 157.0$ (C2), 150.0 (C12), 149.6 (C6), 147.6 (C4), 137.1 (C8), 129.4 (C10), 122.7 (C9), 122.1 (C5), 120.0 (C3), 117.5 (C7), 111.5 (C11), 50.7 (C13), 29.4 (C14), 20.3 (C15), 13.7 ppm (C16); UV/Vis (CH$_2$Cl$_2$): λ_{max} (ε) = 446 nm (135 000 L mol^{-1} cm^{-1}); λ_{MLCT} (ε) = 513 nm (145 000 L mol^{-1} cm^{-1}); TGA: Td$_5$ = 360 °C, Td$_{10}$ = 385 °C; elemental analysis calcd (%) for C$_{126}$H$_{162}$N$_{12}$P$_2$F$_{12}$Ru$\cdot$4 H$_2$O: C 65.58, H 7.42, N 7.28; found: C 65.63, H 7.26, N 6.96.

[Ru(a)$_3$][TRISPHAT]$_2$ (2a): In a Schlenk flask, [RuCl$_2$(dmso)$_4$] (48.3 mg, 0.10 mmol) and ligand **a** (185 mg, 0.3 mmol) were dissolved in ethanol (15 mL). The white suspension turned red upon heating under reflux for 10 h. After cooling to room temperature, [HNBu$_3$][TRISPHAT] (189 mg, 0.2 mmol) was added, and the solution was stirred for 1 h. After precipitation in water (200 mL), the red solid was filtered off, washed with pentane and dried under vacuum. The solvent was evaporated and the product was filtered through a column of silica gel (eluent: CH$_2$Cl$_2$). After evaporation of the solvent under vacuum, the product was recovered as a red powder (120 mg, 34 %). ^{1}H NMR (CD$_2$Cl$_2$): $\delta = 8.48$ (s, 6H; H3), 8.33 (d, $^3J(H,H) = 6$ Hz, 6H; H6), 7.42 (d, 12H; $^3J(H,H) = 9$ Hz, H10), 7.21 (d, $^3J(H,H) = 6$ Hz, 6H; H5), 7.18 (d, $^3J(H,H) = 16.1$ Hz, 6H; H8), 6.93 (d, $^3J(H,H) = 9$ Hz, 12H; H11), 6.75 (d, $^3J(H,H) = 16.1$ Hz, 6H; H7), 4.03 (t, $^3J(H,H) = 6.5$ Hz, 12H; H13), 1.82 (m, 12H; H14), 1.5–1.2 (m, 60H; H15–19), 0.92 ppm (t, $^3J(H,H) = 6.5$ Hz, 18H; H20); ^{13}C NMR (CD$_2$Cl$_2$): $\delta = 160.6$ (C4), 156.9 (C2), 151.6 (C6), 146.4 (C12), 141.5 (d, $J(C,P) = 6$ Hz; TRISPHAT), 135.5 (C8), 129.1 (C10), 127.6 (C9), 122.9 (TRISPHAT), 122.8 (C7), 120.3 (C3 and C5), 114.7 (C11), 114.0 (d, $J(C,P) = 19$ Hz; TRISPHAT), 68.1 (C13), 31.7 (C14), 29.3 (C15), 29.2 (C16), 29.1 (C17), 25.9 (C18), 22.6 (C19), 13.8 ppm (C20); ^{31}P NMR (CD$_2$Cl$_2$): $\delta = -80.6$ ppm; UV/Vis (CH$_2$Cl$_2$): λ_{max} (ε) = 387 nm (124 000 L mol^{-1} cm^{-1}); λ_{MLCT} (ε) = 510 nm (51 000 L mol^{-1} cm^{-1}); emission (CH$_2$Cl$_2$): λ_{em} = 678 nm; TGA: Td$_5$ = 355 °C, Td$_{10}$ = 365 °C; elemental analysis calcd (%) for C$_{162}$H$_{15}$N$_6$O$_{18}$Cl$_{24}$P$_2$Ru: C 55.77, H 4.51, N 2.41; found: C 56.28, H 4.71, N 2.24.

[Fe(a)$_3$][TRISPHAT]$_2$ (3a): Unclean [Fe(**a**)$_3$][PF$_6$]$_2$ (175 mg, 0.08 mmol), resulting from the reaction between FeCl$_2$ and **a** (3 equiv) in refluxing methanol (10 mL), followed by anion exchange with NaPF$_6$, was dissolved in CH$_2$Cl$_2$ (10 mL) in a round-bottom flask. [HNBu$_3$][TRISPHAT] (152 mg, 0.16 mmol) was added, and the greenish solution was stirred for 2 h. The solvent was evaporated, and the product was filtered through a column of silica gel (eluent: CH$_2$Cl$_2$). After evaporation of the solvent under vacuum and recrystallisation from CH$_2$Cl$_2$/pentane (1:10), the product was recovered as a yellow powder (90 mg, 32 %). ^{1}H NMR (CD$_2$Cl$_2$): $\delta = 8.52$ (s, 6H; H3), 7.95 (d, $^3J(H,H) = 6$ Hz, 6H; H6), 7.42 (d, $^3J(H,H) = 8.6$ Hz, 12H; H10), 7.25 (d, $^3J(H,H) = 6$ Hz, 6H; H5), 7.22 (d, $^3J(H,H) = 16.2$ Hz, 6H; H8), 6.94 (d, $^3J(H,H) = 8.6$ Hz, 12H; H11) 6.76 (d, $^3J(H,H) = 16.2$ Hz, 6H; H7), 4.04 (t, $^3J(H,H) = 6.5$ Hz, 12H; H13), 1.82 (m, 12H; H14), 1.5–1.2 (m, 60H; H15–19), 0.92 ppm (t, $^3J(H,H) = 6.5$ Hz, 18H; H20); ^{13}C NMR (CD$_2$Cl$_2$): $\delta = 160.6$ (C4), 159.1 (C2), 154.2 (C6), 147.4 (C12), 141.5 (d, $J(C,P) = 6$ Hz; TRISPHAT), 135.7 (C8), 129.1 (C10), 127.5 (C9), 122.8 (C7, TRISPHAT), 120.2 and 120.0 (C3 or C5), 114.8 (C11), 114.6 (d, $J(C,P) = 19$ Hz; TRISPHAT), 68.2 (C13), 31.8 (C14), 29.3 (C15), 29.2 (C16), 29.1 (C17), 25.9 (C18), 22.7 (C19),

13.9 ppm (C20); ^{31}P NMR (CD$_2$Cl$_2$): $\delta = -80.6$ ppm; UV/Vis (CH$_2$Cl$_2$): λ_{max} (ε) = 382 nm (141 000 Lmol^{-1}cm^{-1}), λ_{MLCT} (ε) = 583 nm (41 000 Lmol^{-1}cm^{-1}); emission (CH$_2$Cl$_2$): λ_{em} = 500 nm; TGA: Td$_5$ = 340°C, Td$_{10}$ = 360°C, elemental analysis calcd (%) for C$_{162}$H15$_6$N$_6$O$_{18}$Cl$_{24}$P$_2$Fe: C 56.50, H 4.57, N 2.44; found: C 57.22, H 4.83, N 2.37.

General procedure for the preparation of metal tris(bipyridyl) complexes [M(b)$_3$][PF$_6$]$_2$: The metal dichloride (0.3 mmol) and ligand **b** (3 equiv, 0.554 g, 0.9 mmol) were dissolved in ethanol (30 mL). The mixture was heated at reflux for 15 h. After the solution had cooled to room temperature, a solution of NaPF$_6$ (0.12 g, 0.7 mmol) in water (20 mL) was added. The resulting precipitate was dissolved in CH$_2$Cl$_2$, and this solution was washed twice with water and then dried over MgSO$_4$. After purification by precipitation with CH$_2$Cl$_2$/pentane (v/v = 1:10), the solvent was removed under vacuum to afford the desired complex in good yield.

[Fe(b)$_3$][PF$_6$]$_2$ (3b): Dark powder, 96% yield; ^{1}H NMR (CD$_2$Cl$_2$): δ = 8.43 (br s, 6H; H3), 7.54 (d, [3]J(H,H) = 16.1 Hz, 6H; H8), 7.49 (d, [3]J(H,H) = 8.9 Hz, 12H; H10), 7.34 (d, [3]J(H,H) = 6.1, 6H; H6), 7.24 (d, [3]J(H,H) = 6.1 Hz, 6H; H5), 6.96 (d, [3]J(H,H) = 16.1 Hz, 6H; H7), 6.68 (d, [3]J(H,H) = 8.9 Hz, 12H; H11), 3.30 (t, [3]J(H,H) = 7.4 Hz, 24H; H13), 1.44 (m, 24H; H14), 1.3 (m, 24H; H15), 0.94 ppm (t, [3]J(H,H) = 7.3 Hz, 36H; H16); ^{13}C NMR (CD$_2$Cl$_2$): δ = 159.2 (C2), 152.4 (C6), 149.6 (C12), 148.5 (C4), 137.4 (C8), 129.5 (C10), 122.8 (C5), 122.1 (C9), 119.7 (C3), 117.4 (C7), 111.6 (C11), 50.7 (C13), 29.4 (C14), 20.3 (C15), 13.8 ppm (C16); UV/Vis (CH$_2$Cl$_2$): λ_{max} (ε) = 467 nm (168 000 Lmol^{-1}cm^{-1}); λ_{MLCT} (ε) = 593 nm (75 000 Lmol^{-1}cm^{-1}); TGA: Td$_5$ = 330°C, Td$_{10}$ = 350°C; HRMS: calcd for C$_{84}$H$_{108}$N$_8$FFe [Fe(**b**)$_2$F]$^+$: 1303.8030, found: 1303.8123; elemental analysis calcd (%) for C$_{126}$H$_{162}$N$_{12}$P$_2$F$_{12}$Fe: C 65.17, H 7.10, N 7.13; found: C 65.67, H 7.41, N 7.01.

[Hg(b)$_3$][PF$_6$]$_2$ (4b): ^{1}H NMR: δ = 8.22 (d, [3]J(H,H) = 5.2 Hz, 6H; H6), 8.15 (s, 6H; H3), 7.54 (d, [3]J(H,H) = 8.4 Hz, 12H; H10), 7.53 (d, [3]J(H,H) = 16.1 Hz, 6H; H8), 7.2 (d, [3]J(H,H) = 5.2 Hz, 6H; H5), 6.78 (d, [3]J(H,H) = 16.1 Hz, 6H; H7), 6.67 (d, [3]J(H,H) = 8.4 Hz, 12H; H11), 3.34 (t, [3]J(H,H) = 7.6 Hz, 24H; H13), 1.61 (m, 24H; H14), 1.41 (m, 24H; H15), 0.99 ppm (t, [3]J(H,H) = 7.3 Hz, 36H; H16); ^{13}C NMR δ = 150.0 (C2), 149.5 and 149.2 (C12 or C4), 148.9 (C6), 137.2 (C8), 129.4 (C10), 122.30 (C9), 122.0 (C5), 118.6 (C3), 118.0 (C7), 111.5 (C11), 50.7 (C13), 29.4 (C14), 20.3 (C15), 13.7 ppm (C16); UV/Vis (CH$_2$Cl$_2$): λ_{max} (ε) = 438 nm (160 000 Lmol^{-1}cm^{-1}).

4,4′-Bis(N,N-diethylaminostyryl)-6,6′-dimethyl-2,2′-bipyridine (a′): nBuLi (1.6 M in hexane, 8.75 mL, 14 mmol) by means of a syringe was added to a solution of diisopropylamine (2 mL, 14 mmol) in THF (10 mL) at −20°C, and the resulting solution was stirred for 15 min. A solution of 4,4′,6,6′-tetramethyl-2,2′-bipyridine (1.5 g, 7 mmol) in THF (30 mL) was added dropwise at −20°C, and the brown-red mixture was stirred for 2 h at this temperatures. A solution of N,N-diethylaminobenzaldehyde (2.53 g, 14 mmol) in THF (20 mL) was slowly added at −20°C. The resulting yellow-green solution was stirred for 2 h at −20°C and then allowed to reach room temperature overnight. After hydrolysis with water (20 mL) and extraction with CH$_2$Cl$_2$ (3 × 50 mL), the organic layers were dried over MgSO$_4$ and filtered, and the solvent was removed under vacuum. The resulting yellow oil was dissolved in toluene (150 mL). After addition of a catalytic amount of PPTS (0.18 g, 0.7 mmol), the red mixture was stirred under reflux during 4 h in a Dean–Stark apparatus. After evaporation of toluene, the residue was dissolved in CH$_2$Cl$_2$ (150 mL) and washed with a saturated aqueous solution of NaHCO$_3$ (3 × 25 mL). The organic layer was dried over MgSO$_4$ and filtered, and the solvent was removed. After recrystallization from 2-methoxyethanol, the desired compound was obtained as a yellow microcrystalline powder (2.0 g, 55%). M.p. 188°C; ^{1}H NMR (300.13 MHz, CDCl$_3$): δ = 8.22 (br s, 2H; H3), 7.43 (d, [3]J(H,H) = 8.8 Hz, 4H; H10), 7.34 (d, [3]J(H,H) = 16.2 Hz, 2H; H8), 7.21 (d, [4]J(H,H) = 1 Hz, 2H; H5), 6.87 (d, [3]J(H,H) = 16.2 Hz, 2H; H7), 6.67 (d, [3]J(H,H) = 8.8 Hz, 4H; H11), 3.39 (q, [3]J(H,H) = 7 Hz, 8H; H13), 2.65 (s, 6H; Me6), 1.18 ppm (t, [3]J(H,H) = 7 Hz, 12H; H14); ^{13}C NMR (75.47 MHz, CDCl$_3$): δ = 158.0 (C6), 156.5 (C2), 148.0 (C12), 146.8 (C4), 133.0 (C8), 128.6 (C10), 123.7 (C9), 121.3 (C7), 119.7 (C5), 115.5 (C3), 111.6 (C11), 44.5 (C13), 24.8 (Me6), 12.7 ppm (C14); UV/Vis (CH$_2$Cl$_2$): λ_{max} (ε) = 391 nm (52 000 Lmol^{-1}cm^{-1}); emission (CH$_2$Cl$_2$): λ_{em} = 497 nm; TGA: Td$_5$ = 305°C, Td$_{10}$ = 330°C; HRMS (FAB): calcd for C$_{36}$H$_{42}$N$_4$ [M]$^+$: 530.3409; found: 530.3442; elemental analysis calcd (%) for C$_{36}$H$_{42}$N$_4$: C 81.47, H 7.98, N 10.56; found: C 81.20, H 8.02, N 10.50.

4,4′-Bis(N,N-dibutylaminostyryl)-6,6′-dimethyl-2,2′-bipyridine (b′): Following the previous procedure, compound **b′** was obtained from 4,4′,6,6′-tetramethyl-2,2′-bipyridine (1.1 g, 5 mmol) and 4-(N,N-dibutylamino)benzaldehyde (2.3 g, 10 mmol) as a yellow-orange microcrystalline powder after recrystallization from ethanol (2.41 g, 75%). M.p. 147°C; ^{1}H NMR (300.13 MHz, CDCl$_3$): δ = 8.22 (br s, 2H; H3), 7.42 (d, [3]J(H,H) = 8.8 Hz, 4H; H10), 7.34 (d, [3]J(H,H) = 16.2 Hz, 2H; H8), 7.21 (d, [4]J(H,H) = 1 Hz, 2H; H5), 6.86 (d, [3]J(H,H) = 16.2 Hz, 2H; H7), 6.63 (d, [3]J(H,H) = 8.8 Hz, 4H; H11), 3.30 (t, [3]J(H,H) = 7 Hz, 8H; H13), 2.66 (s, 6H; Me6), 1.61 (m, 8H; H14), 1.35 (m, 8H; H15), 0.96 ppm (t, [3]J(H,H) = 7.2 Hz, 12H; H16); ^{13}C NMR (75.47 MHz, CD$_2$Cl$_2$): δ = 157.9 (C6), 156.2 (C2), 148.6 (C12), 146.7 (C4), 132.9 (C8), 128.5 (C10), 123.4 (C9), 121.0 (C7), 119.6 (C5), 114.93 (C3), 111.6 (C11), 50.8 (C13), 29.5 (C14), 24.5 (Me6), 20.4 (C15), 13.9 ppm (C16); UV/Vis (CH$_2$Cl$_2$): λ_{max} (ε) = 397 nm (61 000 Lmol^{-1}cm^{-1}); emission (CH$_2$Cl$_2$): λ_{em} = 497 nm; TGA: Td$_5$ = 325°C, Td$_{10}$ = 365°C; HRMS (FAB): calcd for C$_{44}$H$_{58}$N$_4$ [M]$^+$: 642.4661; found: 642.4641; elemental analysis calcd (%) for C$_{44}$H$_{58}$N$_4$·C$_2$H$_5$OH: C 80.18, H9.36, N 8.13; found: C 80.50, H 9.23, N 8.19.

4,4′-Bis(p-(N-methyl-N-octylaminostyryl)-6,6′-dimethyl-2,2′-bipyridine (c′): Following the previous procedure, **c′** was obtained from 4,4′,6,6′-tetramethyl-2,2′-bipyridine (1.1 g, 5 mmol) and 4-(N-methyl-N-octylamino)benzaldehyde (2.5 g, 10 mmol) as a yellow-orange microcrystalline powder after recrystallization from ethanol (2.0 g, 60%). M.p. 142°C; ^{1}H NMR (300.13 MHz, CDCl$_3$): δ = 8.23 (d, [4]J(H,H) = 1.1 Hz, 2H; H3), 7.44 (d, [3]J(H,H) = 8.8 Hz, 4H; H10), 7.35 (d, [3]J(H,H) = 16.2 Hz, 2H; H8), 7.21 (d, [4]J(H,H) = 1.1 Hz, 2H; H5), 6.88 (d, [3]J(H,H) = 16.2 Hz, 2H; H7), 6.67 (d, [3]J(H,H) = 8.8 Hz, 4H; H11), 3.34 (t, [3]J(H,H) = 7.5 Hz, 8H; H13), 2.97 (s, 6H; H13′), 2.66 (s, 6H; Me6), 1.59 (m, 4H; H14), 1.27 (m, 20H; H15–19), 0.88 ppm (t, [3]J(H,H) = 6.6 Hz, 6H; H20); ^{13}C NMR (75.47 MHz, CDCl$_3$, 297 K): δ = 157.9 (C6), 156.5 (C2), 149.5 (C12), 146.7 (C4), 133.0 (C8), 128.4 (C10), 124.2 (C9), 121.6 (C7), 119.6 (C5), 115.5 (C3), 111.8 (C11), 52.6 (C13), 38.3 (C13′) 31.8 (C14), 29.5 (C15), 29.3 (C16), 27.2 (C17), 26.8 (C18), 24.7 (Me6), 22.6 (C19), 14.1 ppm (C20); UV/Vis (CH$_2$Cl$_2$): λ_{max} (ε) = 386 nm (49 000 Lmol^{-1}cm^{-1}); HRMS (FAB): calcd for C$_{46}$H$_{62}$N$_4$ [M]$^+$: 670.4974; found: 670.4971; elemental analysis calcd (%) for C$_{46}$H$_{62}$N$_4$·C$_2$H$_5$OH: C 80.40, H 9.56, N 7.81; found: C 80.52, H 9.12, N 8.25.

General procedure for the synthesis of copper complexes: [Cu(CH$_3$CN)$_4$][PF$_6$] (92 mg, 0.25 mmol) and the corresponding bipyridyl ligand (0.5 mmol) were dissolved in CH$_2$Cl$_2$ (20 mL) in a Schlenk vessel. The mixture instantaneously turned red and was stirred overnight. After evaporation of the solvent, the desired complex was precipitated from CH$_2$Cl$_2$/diethyl ether (v/v = 1:10). The resulting microcrystalline solid was filtered, washed with pentane, and dried under vacuum.

[Cu(a′)$_2$][PF$_6$] (5a′): Red-orange complex (90%); ^{1}H NMR (300.13 MHz, CD$_2$Cl$_2$): δ = 8.16 (s, 4H; H3), 7.48 (d, [3]J(H,H) = 8.8 Hz, 8H; H10), 7.46 (d, [3]J(H,H) = 16.1 Hz, 4H; H8), 7.42 (s, 4H; H5), 6.92 (d, [3]J(H,H) = 16.1 Hz, 4H; H7), 6.69 (d, [3]J(H,H) = 8.8 Hz, 8H; H11), 3.40 (q, [3]J(H,H) = 7.0 Hz, 16H; H13), 2.22 (s, 12H; Me6), 1.18 ppm (t, [3]J(H,H) = 7.0 Hz, 24H; H14); UV/Vis (CH$_2$Cl$_2$): λ_{max} (ε) = 433 (83 000 Lmol^{-1}cm^{-1}), λ_{MLCT} (ε) = 482 (40 000 Lmol^{-1}cm^{-1}); HRMS (FAB): calcd for CuC$_{72}$H$_{84}$N$_8$ [M]$^+$: 1123.6115; found: 1123.6157; elemental analysis calcd (%) for CuC$_{72}$H$_{84}$N$_8$PF$_6$·2 CH$_2$Cl$_2$: C 61.73, H 6.16, N 7.78; found: C 61.98, H 6.60, N 7.37.

[Cu(b′)$_2$][PF$_6$] (5b′): Red-orange product (91%); ^{1}H NMR (300.13 MHz, CD$_2$Cl$_2$): δ = 8.16 (s, 4H; H3), 7.47 (d, [3]J(H,H) = 8.8 Hz, 8H; H10), 7.45 (d, [3]J(H,H) = 16.1 Hz, 4H; H8), 7.41 (s, 4H; H5), 6.92 (d, [3]J(H,H) = 16.1 Hz, 4H; H7), 6.66 (d, [3]J(H,H) = 8.8 Hz, 8H; H11), 3.31 (t, [3]J(H,H) = 7.5 Hz, 16H; H13), 2.21 (s, 12H; Me6), 1.55 (m, 16H; H14), 1.35 (m, 16H; H15), 0.96 ppm (t, [3]J(H,H) = 7.2 Hz, 24H; H16); ^{13}C NMR (75.47 MHz, CD$_2$Cl$_2$): δ = 156.8 (C6), 152.6 (C4), 149.4 (C12), 148.2 (C2), 135.8 (C8), 129.5 (C10), 123.2 (C9), 121.6 (C5), 119.7 (C3), 116.7 (C7), 112.0 (C11), 51.2 (C13), 29.9 (C14), 25.6 (Me6), 20.7 (C15), 14.5 ppm (C16); ^{31}P NMR (121.49 MHz, CD$_2$Cl$_2$): δ = −143.9 ppm (hept, [2]J(P,F) = 710 Hz; PF$_6$); UV/Vis (CH$_2$Cl$_2$): λ_{max} (ε) = 436 nm (106 000 Lmol^{-1}cm^{-1}); λ_{MLCT} (ε) = 480 nm (45 000 Lmol^{-1}cm^{-1}); TGA: Td$_5$ = 310°C, Td$_{10}$ = 340°C; HRMS (FAB): calcd for CuC$_{88}$H$_{116}$N$_8$: [M]$^+$ 1347.8619; found: 1347.8600; elemental analysis calcd (%) for CuC$_{88}$H$_{116}$N$_8$PF$_6$·$\frac{1}{2}$ CH$_2$Cl$_2$: C 69.16, H 7.67, N 7.29; found: C 69.16, H 7.55, N 7.10.

Acknowledgements

[1] a) T. Verbiest, S. Houbrechts, M. Kauranen, K. Clays, A. Persoons, *J. Mater. Chem.* **1997**, *7*, 2175–2189; b) N. J. Long, *Angew. Chem.* **1995**, *107*, 37–56; *Angew. Chem. Int. Ed. Engl.* **1995**, *34*, 21–38; c) T. J. Marks, M. A. Ratner, *Angew. Chem.* **1995**, *107*, 167–187; *Angew. Chem. Int. Ed. Engl.* **1995**, *34*, 155–173; d) H. Le Bozec, T. Renouard, *Eur. J. Inorg. Chem.* **2000**, 229–239.

[2] J. Zyss, I. Ledoux, *Chem. Rev.* **1994**, *94*, 77–105.

[3] For a review, see: O. Riant, G. Bluet, S. Brasselet, N. Druze, I. Ledoux, F. Lefloch, A. Skibniewski, J. Zyss, *Mol. Cryst. Liq. Cryst.* **1998**, *322*, 35–42.

[4] a) I. Ledoux, J. Zyss, J. S. Siegel, J. Brienne, J. M. Lehn, *Chem. Phys. Lett.* **1990**, *172*, 440–444; b) T. Verbiest, K. Clays, C. Semyr, J. Wolff, D. Reihoudt, A. Persoons, *J. Am. Chem. Soc.* **1994**, *116*, 9320–9323; c) J. L. Bredas, F. Meyers, B. M. Pierce, J. Zyss, *J. Am. Chem. Soc.* **1992**, *114*, 4928–4929; d) J. J. Wolff, D. Längle, D. Hillenbrand, R. Wortmann, R. Matschiner, C. Glania, P. Krämer, *Adv. Mater.* **1997**, *9*, 138–143; e) R. Wortmann, C. Glania, P. Krämer, R. Matschiner, J. J. Wolff, S. Kraft, B. Treptow, E. Barbu, D. Längle, G. Görlitz, *Chem. Eur. J.* **1997**, *3*, 1765–1773; f) C. Lambert, G. Nöll, E. Schmälzlin, K. Meerholz, C. Bräuchle, *Chem. Eur. J.* **1998**, *4*, 2129–2135; g) B. R. Cho, S. K. Lee, K. A. Kim, K. N. Son, T. I. Kang, S. J. Jeon, *Tetrahedron Lett.* **1998**, *39*, 9205–9208; h) A. M. McDonagh, M. G. Humphrey, M. Samoc, B. Luther-Davies, S. Houbrechts, T. Wada, H. Sasabe, A. Persoons, *J. Am. Chem. Soc.* **1999**, *121*, 1405–1406; i) C. Andraud, T. Zabulon, A. Collet, J. Zyss, *Chem. Phys.* **1999**, *245*, 243–261; j) A. Omenat, J. Barbera, J. L. Serrano, S. Houbrechts, A. Persoons, *Adv. Mater.* **1999**, *11*, 1292–1295; k) B. R. Cho, S. J. Lee, S. H. Lee, K. H. Son, Y. H. Kim, I.-Y. Doo, G. J. Lee, T. I. Kang, Y. K. Lee, M. Cho, S.-J. Jeon, *Chem. Mater.* **2001**, *13*, 1438–1440; l) J. Brunel, I. Ledoux, J. Zyss, M. Blanchard-Desce, *Chem. Commun.* **2001**, 923–924; m) B. R. Cho, S. B. Park, S. J. Lee, K. H. Son, S. H. Lee, M.-J. Lee, J. Yoo, Y. K. Lee, G. J. Lee, T. I. Kang, M. Cho, S.-J. Jeon, *J. Am. Chem. Soc.* **2001**, *123*, 6421–6422.

[5] a) S. Brasselet, F. Cherioux, P. Audebert, J. Zyss, *Chem. Mater.* **1999**, *11*, 1915–1920; b) V. R. Thalladi, R. Boese, S. Brasselet, I. Ledoux, J. Zyss, R. K. R. Jetti, G. R. Desiraju, *Chem. Commun.* **1999**, 1639–1640; c) F. Cherioux, H. Maillotte, P. Audebert, J. Zyss, *Chem. Commun.* **1999**, 2083–2084; d) J. J. Wolff, F. Siegler, R. Matschiner, R. Wortmann, *Angew. Chem.* **2000**, *112*, 1494–1498; *Angew. Chem. Int. Ed.* **2000**, *39*, 1436–1439.

[6] G. Alcaraz, L. Euzenat, O. Mongin, C. Katan, I. Ledoux, J. Zyss, M. Blanchard-Desce, M. Vaultier, *Chem. Commun.* **2003**, 2766–2767.

[7] For carbocations, see: a) J. Zyss, T. Chauvan, C. Dhenaut, I. Ledoux, *Chem. Phys.* **1993**, *177*, 281–296; b) A. Verbiest, K. Clays, C. Samyn, J. Wolff, D. Reinhoudt, A. Persoons, *J. Am. Chem. Soc.* **1994**, *116*, 9320–9323; c) Y.-K. Lee, S.-J. Jeon, M. Cho, *J. Am. Chem. Soc.* **1998**, *120*, 10921–10927. For carbanions, see: T. Verbiest, K. Clays, A. Persoons, F. Meyers, J.-L. Brédas, *Opt. Lett.* **1993**, *18*, 525–527; for carbon radicals, see: I. Ratera, S. Marcen, S. Montant, D. Molina-Ruiz, C. Rovira, J. Veciana, J.-F. Letard, E. Freysz, *Chem. Phys. Lett.* **2002**, *363*, 245–251.

[8] a) S. Stadler, C. Bräuchle, S. Brandl, R. Gompper, *Chem. Mater.* **1996**, *8*, 414–417; b) C. Lambert, W. Gaschler, E. Schmälzlin, K. Meerholz, C. Bräuchle, *J. Chem. Soc. Perkin Trans. 2* **1999**, 577–587.

[9] P. D. Maker, *Phys. Rev. A* **1970**, *1*, 923.

[10] a) C. Bourgogne, Y. Le Fur, P. Juen, P. Masson, J.-F. Nicoud, R. Masse, *Chem. Mater.* **2000**, *12*, 1025–1033; b) C. Lambert, E. Schmälzlin, K. Meerholz, C. Bräuchle, *Chem. Eur. J.* **1998**, *4*, 512–521.

[11] M. Lequan, C. Branger, J. Simon, T. Thami, E. Chauchard, A. Persoons, *Adv. Mater.* **1994**, *6*, 851–853.

[12] a) A. Sastre, T. Torres, M. A. Diaz-Garcia, F. Agullo-Lopez, C. Dhenaut, S. Brasselet, I. Ledoux, J. Zyss, *J. Am. Chem. Soc.* **1996**, *118*, 2746–2747; b) B. del Rey, U. Keller, T. Torres, G. Rojo, F. Agullo-Lopez, S. Nonell, C. Marti, S. Brasselet, I. Ledoux, J. Zyss, *J. Am. Chem. Soc.* **1998**, *120*, 12808–12817.

[13] a) M. Blanchard-Desce, J.-B. Baudin, O. Ruel, L. Jullien, S. Brasselet, J. Zyss, *Opt. Mater.* **1998**, *9*, 276–279; b) M. Blanchard-Desce, J.-B. Baudin, L. Jullien, R. Lorne, O. Ruel, S. Brasselet, J. Zyss, *Opt. Mater.* **1999**, *12*, 333–338.

[14] P. Mukhopadhyay, P. K. Bharadwaj, G. Savitha, A. Krishnan, P. K. Das, *Chem. Commun.* **2000**, 1815–1816.

[15] J. Zyss, I. Ledoux, S. Volkov, V. Cherniak, S. Mukamel, G. P. Bartholomew, G. C. Bazan, *J. Am. Chem. Soc.* **2000**, *122*, 11956–11962.

[16] J. Zyss, C. Dhenaut, T. Chau Van, I. Ledoux, *Chem. Phys. Lett.* **1993**, *206*, 409.

[17] a) W. Lin, Z. Wang, L. Ma, *J. Am. Chem. Soc.* **1999**, *121*, 11249–11250; b) W. Lin, L. Ma, O. R. Evans, *Chem. Commun.* **2000**, 2263–2264; c) O. R. Evans, W. Lin, *Chem. Mater.* **2001**, *13*, 2705–2712; d) O. R. Evans, W. Lin, *Acc. Chem. Res.* **2002**, *35*, 511–522.

[18] a) C. Dhenaut, I. Ledoux, I. D. W. Samuel, J. Zyss, M. Bourgault, H. Le Bozec, *Nature* **1995**, *374*, 339–342; b) T. Renouard, H. Le Bozec, I. Ledoux, J. Zyss, *Chem. Commun.* **1999**, 871–872; c) H. Le Bozec, T. Renouard, M. Bourgault, C. Dhenaut, S. Brasselet, I. Ledoux, J. Zyss, *Synth. Met.* **2001**, *124*, 185–189; d) T. Le Bouder, O. Maury, H. Le Bozec, I. Ledoux, J. Zyss, *Chem. Commun.* **2001**, 2430–2431; e) H. Le Bozec, T. Le Bouder, O. Maury, A. Bondon, J. Zyss, I. Ledoux, *Adv. Mater.* **2001**, *13*, 1677–1681; f) K. Sénéchal, O. Maury, H. Le Bozec, I. Ledoux, J. Zyss, *J. Am. Chem. Soc.* **2002**, *124*, 4561–4562; g) L. Viau, M. Even, O. Maury, D. Haddleton, H. Le Bozec, *Macromol. Rapid Commun.* **2003**, *24*, 630–635; h) T. Le Bouder, O. Maury, H. Le Bozec, A. Bondon, K. Costuas, E. Amouyal, J. Zyss, I. Ledoux, *J. Am. Chem. Soc.* **2003**, *125*, 12884–12899.

[19] O. Maury, J.-P. Guégan, T. Renouard, A. Hilton, P. Dupau, N. Sandon, L. Toupet, H. Le Bozec, *New J. Chem.* **2001**, *25*, 1553–1566.

[20] L. Viau, K. Sénéchal, O. Maury, J.-P. Guégan, P. Dupau, L. Toupet, H. Le Bozec, *Synthesis* **2003**, 577–582.

[21] This ligand was preliminary reported in: L. Viau, O. Maury, H. Le Bozec, *Tetrahedron Lett.* **2004**, *45*, 125–128.

[22] a) J. Lacour, C. Glinglinger, C. Grivet, G. Bernardelli, *Angew. Chem.* **1997**, *109*, 660–662; *Angew. Chem. Int. Ed. Engl.* **1997**, *36*, 608–610; b) O. Maury, J. Lacour, H. Le Bozec, *Eur. J. Inorg. Chem.* **2001**, 201–204, and references therein.

[23] a) A. K.-J. Jen, X. Wu, H. Ma, *Chem. Mater.* **1998**, *10*, 471–473; b) C.-F. Shu, Y.-C. Shu, Z.-H. Gong, S.-M. Peng, G. H. Lee, A. K.-J. Jen, *Chem. Mater.* **1998**, *10*, 3284–3286; c) Y.-C. Shu, Z.-H. Gong, C.-F. Shu, E. M. Breitung, R. J. McMahon, G. H. Lee, A. K.-J. Jen, *Chem. Mater.* **1999**, *11*, 1628–1632; d) X. Wu, J. Wu, Y. Liu, A. K.-J. Jen, *Chem. Commun.* **1999**, 2391–2392; e) J.-M. Raimundo, P. Blanchard, I. Ledoux-Rak, R. Hierle, L. Michaud, J. Roncali, *Chem. Commun.* **2000**, 1597–1598.

[24] HRMS (FAB) for **1b**, fragment [Zn(**b**)$_2$F]$^+$, calcd for C$_{84}$H$_{108}$N$_8$FZn$^+$, *m/z*: 1311.7972 (found 1311.8043). Similar behavior was observed for **3b**.

[25] a) C. O. Dietrich-Bruchecker, J.-P. Sauvage, *Chem. Rev.* **1987**, *87*, 795–810; b) J.-P. Sauvage, *Acc. Chem. Res.* **1990**, *23*, 319–327.

[26] For a complete NMR study in the case of copper complexes, see: A. J. Pallenberg, K. S. Koenig, D. M. Barnhart, *Inorg. Chem.* **1995**, *34*, 2833–2840.

[27] A. J. Pallenberg, T. M. Marsher, D. M. Barnhart, *Polyhedron* **1997**, *16*, 2711–2719.

[28] For Lewis acidity scale of metal chlorides, see S. Kobahashi, T. Busujima, S. Nagamaya, *Chem. Eur. J.* **2000**, *6*, 3491–3494.

[29] M. H. Ford-Smith, N. Sutin, *J. Am. Chem. Soc.* **1961**, *83*, 1830.

[30] F. W. Vance, J. T. Hupp, *J. Am. Chem. Soc.* **1999**, *121*, 4047–4053.

[31] T. Renouard, PhD Thesis of Rennes I University, **1998**.

[32] M. J. Cook, A. P. Lewis, G. S. G. McAuliffe, V. Skarda, A. J. Thomson, J. L. Glasper, D. J. Robbins, *J. Chem. Soc. Perkin Trans. 2* **1984**, 1293–1301.

[33] For a recent review, see N. Armaroli, *Chem. Soc. Rev.* **2001**, *30*, 113–124, and references therein; for recent examples, see E. C. Constable, C. E. Housecroft, M. Neuburger, I. Poleschak, M. Zehnder, *Polyhedron* **2003**, *22*, 93–108.

[34] a) R. W. Terhune, P. D. Maker, C. M. Savage, *Phys. Rev.* **1965**, *14*, 681; b) K. Clays, A. Persoons, *Phys. Rev. Lett.* **1991**, *66*, 2980.

[35] I. D. Morrison, R. G. Denning, W. M. Laidlaw, M. A. Stammers, *Rev. Sci. Instrum.* **1996**, *67*, 1445.

[36] a) M. Cho, H.-S. Kim, S.-J. Jeon, *J. Chem. Phys.* **1998**, *108*, 7114–7120; b) Y.-K. Lee, S.-J. Jeon, M. Cho, *J. Am. Chem. Soc.* **1998**, *120*, 10921–10927; c) H. Lee, S.-Y. An, M. Cho, *J. Phys. Chem. B* **1999**, *103*, 4992–4996.

[37] Some complexes were prepared with TRISPHAT as the counteranion, and it is worth noting that this anion is also octupolar (D_3). The quadratic hyperpolarizability of [HNBu$_3$][TRISPHAT] was measured by harmonic light scattering at $\lambda = 1.064$ μm ($\beta^{1.064} = 9 \times 10^{-30}$ esu). Since this NLO activity is one order of magnitude lower than those of the cations, its contribution to the global NLO activity can be considered to be negligible.

[38] a) V. P. Rao, A.-K. Jen, K. Y. Wong, K. J. Drost, *Tetrahedron Lett.* **1993**, *34*, 1747–1750; b) A.-K. Jen, V. P. Rao, K. Y. Wong, K. J. Drost, *J. Chem. Soc. Chem. Commun.* **1993**, 90–92; c) A.-K. Jen, Y. Cai, P. V. Bedworth, S. R. Marder, *Adv. Mater.* **1997**, *9*, 132–135; d) V. P. Rao, A.-K. Jen, K. Y. Wong, K. J. Drost, *J. Chem. Soc. Chem. Commun.* **1993**, 1118–1110; e) X. Wu, J. Wu, Y. Liu, A.-K. Jen, *J. Am. Chem. Soc.* **1999**, *121*, 472–473; f) V. P. Rao, A. K.-Y. Jen, Y. Cai, *Chem. Commun.* **1996**, 1237–1238.

[39] T. L. Gilchrist, *Heterocycle Chemistry*, Wiley, New York, **1985**.

[40] a) I. D. L. Albert, T. J. Marks, M. A. Ratner, *J. Am. Chem. Soc.* **1997**, *119*, 6575–6582; b) E. M. Breitung, C.-F. Shu, R. J. McMahon, *J. Am. Chem. Soc.* **2000**, *122*, 1154–1160.

[41] a) A. Hilton, T. Renouard, O. Maury, H. Le Bozec, I. Ledoux, J. Zyss, *Chem. Commun.* **1999**, 2521–2522; b) I. R. Whittall, M. G. Humphrey, A. Persoons, S. Houbrechts, *Organometallics* **1996**, *15*, 1935–1941; c) I. R. Whittall, M. G. Humphrey, S. Houbrechts, A. Persoons, D. C. Hockless, *Organometallics* **1996**, *15*, 5738–5745; d) for C=C containing chromophores, see: S.-S. P. Chou, D.-J. Sun, J. Y. Huang, P.-K. Yang, H. C. Lin, *Tetrahedron Lett.* **1996**, *37*, 7279–7282; e) for related imino molecules, see: S.-S. P. Chou, D.-J. Sun, H. C. Lin, P.-K. Yang, *Chem. Commun.* **1996**, 1045–1046.

[42] T. Tsunekawa, K. Yamaguchi, *J. Phys. Chem.* **1992**, *96*, 10268–10275.

[43] The oscillator strength f was calculated with the following relationship: $f = 4.319 \times 10^{-9} \times \varepsilon \times \nu_{1/2}$ where $\nu_{1/2}$ represents the half-height bandwidth (cm^{-1}): $f = 1.97$ (**6b′**, M = Ag) and 1.90 (**1b′**, M = Zn). In the case of **5b′** (M = Cu), f could not be determined on account of an overlap between both ILCT and MLCT transitions.

[44] I. P. Evans, A. Spencer, G. Wilkinson, *J. Chem. Soc. Dalton Trans.* **1973**, 204–209.

[45] J. Zyss, J.-F. Nicoud, M. Coquillay, *J. Chem. Phys.* **1984**, *81*, 4160.

[46] S. G. Yan, J. T. Hupp, *J. Phys. Chem.* **1996**, *100*, 6867–6870.